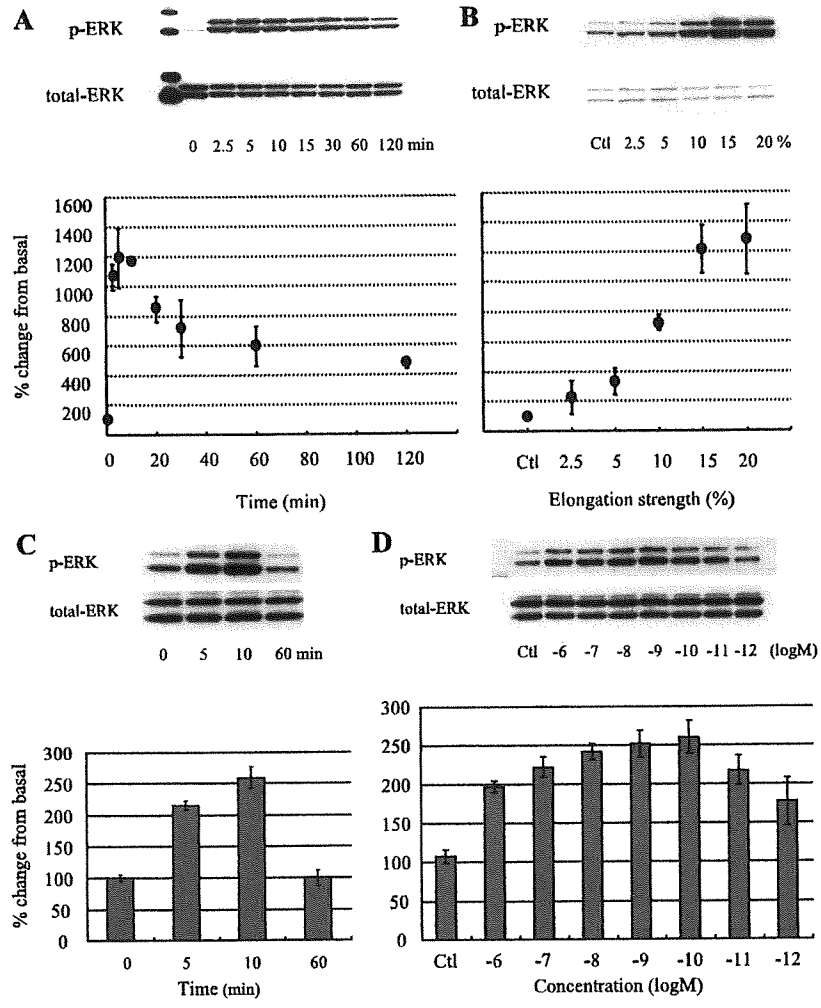

Fig. 1. Mechanical strain and angiotensin II (Ang II) induce the activation of ERK in a time-dependent and elongation strength (dose)-dependent manner. Phosphorylation (p) levels of ERK were expressed as % change from the control. *A*: increase in p-ERK by stretch was time dependent; maximal response was obtained at 5 min after the initiation of stretch. *B*: increase in p-ERK by stretch was elongation strength dependent; maximal response was obtained with 20% elongation. The increase in p-ERK by Ang II was time dependent (*C*) and concentration dependent (*D*). Ang II concentration of 10^{-10} M was used for the time-course study, and an incubation time of 10 min was used for the dose-response study. The maximal response was obtained with 10^{-10} M of Ang II at an incubation time of 10 min. Means ± SE (n = 4) are given. Ctl, control.

manner (□, EC_{50} = 1.3 × 10^{-8} M, maximal inhibition, 50.6 ± 11.0% at 10^{-5} M) with olmesartan treatment. In contrast, olmesartan did not have a significant inhibitory effect on the activation of ERK at 5 min of mechanical stress when maximal p-ERK activation was obtained by mechanical strain (Fig. 2*A*, ●). Because ERK was only minimally active at basal conditions without added Ang II in RMCs, olmesartan did not significantly affect the basal phosphorylation levels of ERK (Fig. 2*B*). To compare the effects of two different ARBs, the cells were preincubated with losartan or olmesartan. In contrast to olmesartan, losartan did not show a significant inhibitory effect on the activation of ERK induced by mechanical strain at the plateau phase. Losartan did not change the basal phosphorylation levels of ERK, similar to the result obtained with olmesartan (Fig. 2*B*).

The effect of AT1R blockade by olmesartan was observed only at plateau phase. For this reason, in subsequent studies, the levels of ERK phosphorylation were studied at 60 min of cyclic stretch at 20% elongation. Because several mechanisms have been described as pathways of mechanotransduction in mechanosensitive tissues including the heart, vasculature, and kidney, the rapid activation of ERK not blocked by olmesartan may be mediated by an AT1R-independent pathway. Integrins, interacting with the connecting matrix/environment, mediate increases in intracellular Ca^{2+} levels and activate MAPK cascades to cause ERK phosphorylation. Also, previous reports have implicated a stretch-activated ion channel in mediating mechanotransduction (10).

To determine the autocrine/paracrine effects of Ang II, activation of the renin-angiotensin system was assessed. There were no changes in angiotensinogen mRNA levels following 60 min of cyclic mechanical strain (control: 1.51 ± 0.04; olmesartan only: 1.50 ± 0.05; stretch only: 1.52 ± 0.03; stretch after olmesartan pretreatment: 1.51 ± 0.03, no significant differences among groups; data are expressed as ΔC_t value normalized to β-actin ± SE, n = 6). The concentration of Ang II in the culture medium was below the detection limit using EIA (3 pg/ml) before and 10, 20, 30, and 60 min after application of the mechanical strain. The stimulatory effect of Ang II on ERK peaked at 10 min and disappeared after 60 min (Fig. 1*C*). This result supports our contention that the effects of 60 min of mechanical strain on ERK phosphorylation were not

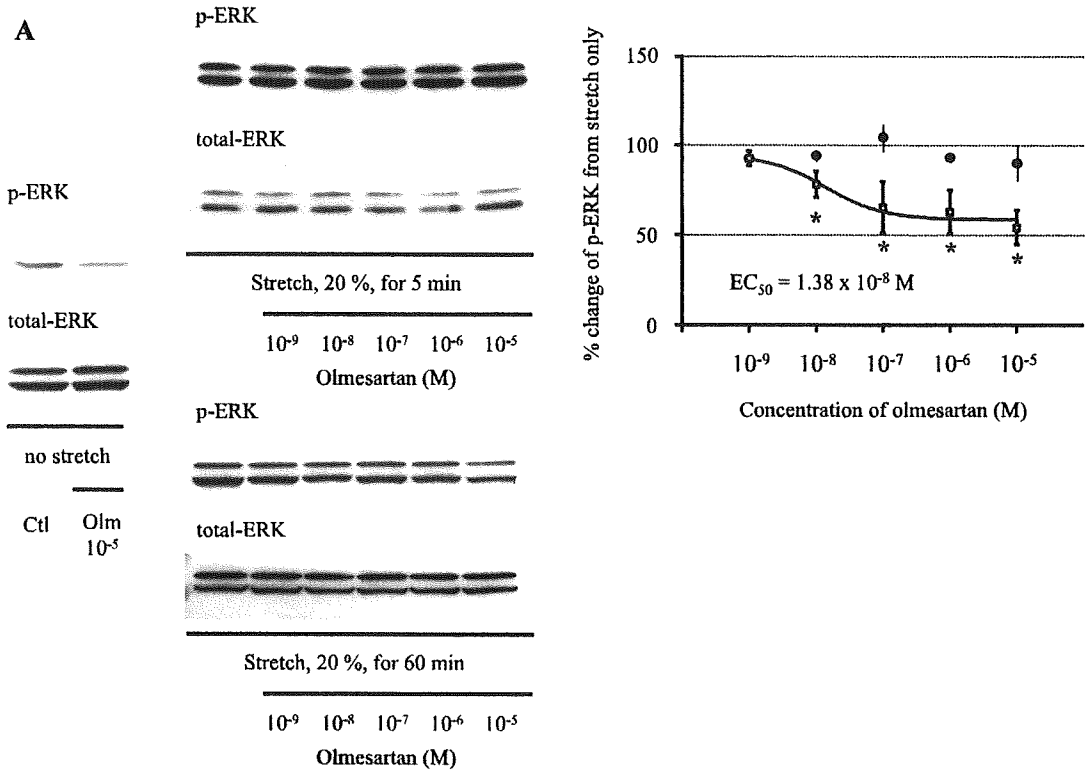

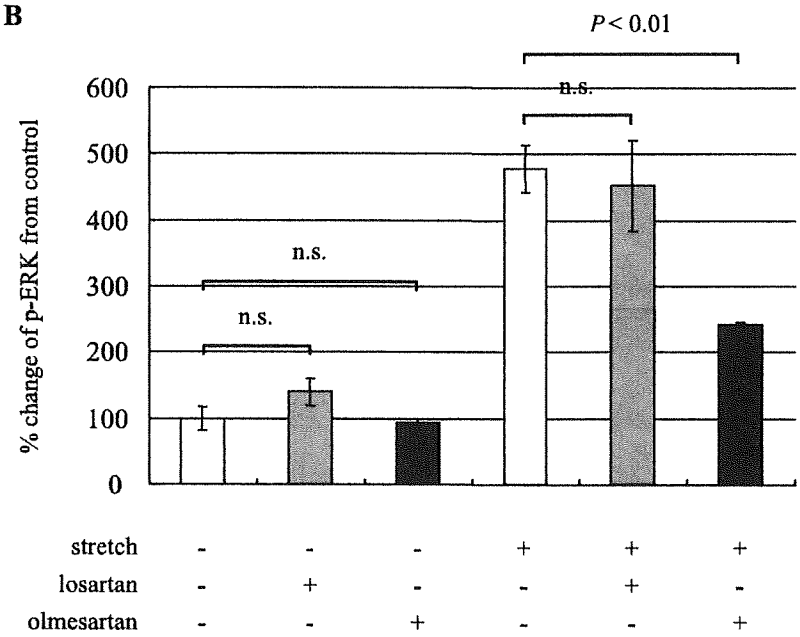

Fig. 2. Effect of mechanical strain and olmesartan on the phosphorylation levels of ERK. *A*: concentration-dependent effect of olmesartan (Olm) on mechanical strain-induced activation of ERK. Phosphorylated ERK levels were expressed as % change from the control. $^*P < 0.01$ vs. control. Means ± SE ($n = 5$) are given. p-ERK levels at the plateau phase (□) were reduced in a concentration-dependent manner ($EC_{50} = 1.3 \times 10^{-8}$ M, maximal inhibition 50.6 ± 11.0% at 10^{-5} M) with olmesartan treatment. In contrast, p-ERK levels at early phase (●) were not attenuated by pretreatment with olmesartan. *B*: olmesartan as well as losartan (10^{-5} M) did not change basal p-ERK levels but attenuated the elevated levels of p-ERK induced by cyclic mechanical strain at plateau phase. In contrast to olmesartan, losartan did not have any inhibitory effect on the stretch-induced ERK activation at the plateau phase of 60 min. Means ± SE ($n = 5$) are given. n.s., not significant.

attributable to an increase in Ang II that was below the detection limit of our method.

Effect of AT1R miRNA on mechanical strain-induced ERK activation. It is possible that the inhibition of stretch-induced p-ERK elevation by olmesartan is independent of AT1R blockade. To further demonstrate that the activation via mechanical strain was transduced through the AT1R even in the absence of Ang II, *Rattus norvegicus* $AT_{1A}R$ gene expression was inhibited using RNA interference (RNAi) technique. miRNA against rat $AT_{1A}R$, which was produced by BLOCK-iT Pol II miRNA RNAi expression vector, decreased protein expression levels of $AT_{1A}R$ by 76.8 ± 6.8% relative to the mock vector-treated control (Fig. 3*A*). $AT_{1A}R$ miRNA treatment attenuated the p-ERK levels at the plateau phase (60 min) (53.5 ± 9.7%, Fig. 3*B*) but did not affect p-ERK levels at the initial peak (5 min) (Fig. 3*C*), corroborating the results obtained with olmesartan.

Involvement of oxidative stress caused by mechanical strain through AT1R. Oxidative stress is known to be involved in the activation of ERK by AT1R. In this study, Tempol, a superoxide dismutase mimetic, also lowered the plateau phase p-ERK levels induced by mechanical strain in a dose-dependent manner (Fig. 4; maximal inhibition of ~50% was obtained at 10^{-5} M). NADPH oxidase is activated by Ang II, and NADPH oxidase-dependent O_2^- and H_2O_2 production transactivate the MAPK cascade via receptor tyrosine kinases (8, 26). Hydrogen peroxide time and concentration dependently stimulated ERK phosphorylation in RMCs (maximal response of 521.6 ± 47.5% increase in ERK phosphorylation from control was obtained with 0.001% H_2O_2 at 60 min; means ± SE, n = 4). Thus, to determine the relationship between mechanical strain-induced activation of ERK through AT1R and NADPH oxidase activity, the translocation of $p47^{phox}$, a cytosolic component of NADPH oxidase, to the cell membrane was examined by Western blotting. The abundance of $p47^{phox}$ in the cell membrane fraction and phosphorylated $p47^{phox}$ in whole cell was significantly increased by mechanical strain (Fig. 5). Olmesartan was able to block the stretch-induced translocation and the serine phosphorylation of $p47^{phox}$.

We also examined the effect of olmesartan on the mRNA expression levels of NADPH oxidase subunits $p22^{phox}$, $p47^{phox}$, $p67^{phox}$, $gp91^{phox}$, Nox-1, and Nox-4 using real-time RT-PCR. The basal expression levels of $p22^{phox}$ and $p67^{phox}$ were significantly decreased after olmesartan treatment (Fig. 6). Cyclic mechanical strain increased the expressions of $p47^{phox}$, $p22^{phox}$, and $p67^{phox}$, and olmesartan attenuated the elevated expression levels. In contrast, cyclic mechanical strain did not

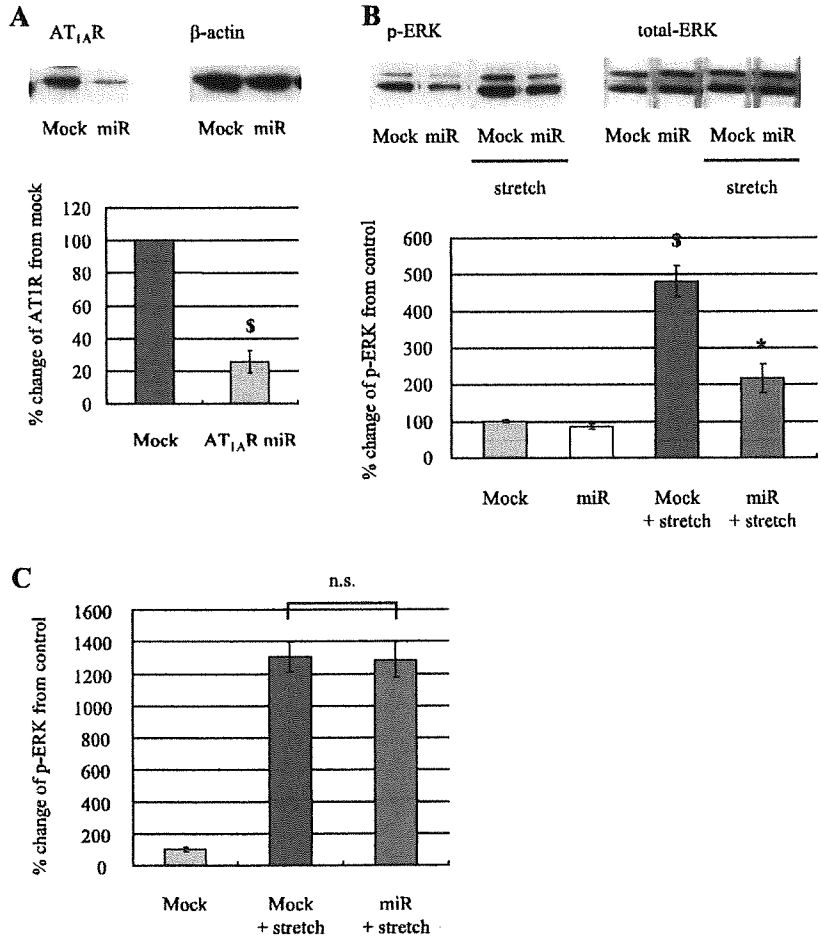

Fig. 3. Effect of micro RNA (miRNA, miR) against Ang II type 1 receptor (AT1R) on ERK phosphorylation induced by mechanical strain. *A*: transfection with miRNA significantly decreased the basal expression levels of AT1R (76.8 ± 6.8% reduction). *B*: miRNA treatment significantly attenuated the stretch-induced elevation of phosphorylation levels of ERK at plateau phase (53.5 ± 9.7% reduction). Means ± SE (n = 3) are given. $\$P < 0.01$ vs. mock control, $*P < 0.01$ vs. mock + stretch. *C*: AT1R silencing did not have any inhibitory effect on ERK phosphorylation at initial peak 5 min after stretch application (1,304.38 ± 93.8% increasing of p-ERK in mock group vs. 1,284.98 ± 111.3% in miR group, n = 4). $AT_{1A}R$, Ang II type 1A receptor.

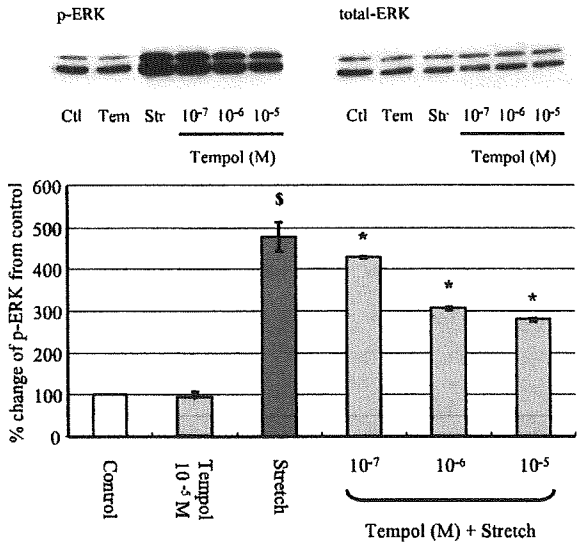

Fig. 4. The effect of Tempol on plateau-phase ERK phosphorylation induced by mechanical strain (Str). Phosphorylation levels of ERK were expressed as % of the control. Similar to the result obtained with olmesartan pretreatment, Tempol dose dependently lowered ERK activity at plateau phase induced by mechanical strain. Maximal inhibition was observed with 10^{-5} M of Tempol (Tem). Means ± SE (n = 3) are given. $\$P < 0.01$ from control; $*P < 0.01$ vs. control.

have any significant effect on the expression levels of gp91^{phox}, Nox-1, and Nox-4.

The effect of BAPTA and cytochalasin D on stretch-induced ERK phosphorylation. Finally, an additional experiment was performed to explore the reason why neither olmesartan nor $AT_{1A}R$ gene silencing had any inhibitory effect on ERK phosphorylation at the rapid phase (5 min) after the initiation of mechanical strain. BAPTA-TM, a potent chelator of calcium ion, and cytochalasin D, an inhibitor of actin polymeration, were used to study the AT1R-induced, oxidative stress-independent activation of ERK (Fig. 7). The early-phase activation of ERK induced by cyclic mechanical strain was abolished almost completely by preincubation with either 1 μM BAPTA-TM or 1 μM cytochalasin D. In contrast, the phosphorylation of ERK at the plateau phase by mechanical strain was still observed with BAPTA-TM or cytochalasin D.

DISCUSSION

This study demonstrates for the first time that mechanical strain increases the phosphorylation levels of ERK in RMCs via AT1R even in the absence of Ang II. An ARB, olmesartan, attenuates ERK activation after 60 min of mechanical strain. This is not due to inhibition of locally de novo synthesized Ang II (13, 20, 21) because the concentrations of secreted Ang II and the expression levels of angiotensinogen are unchanged by stretch. Indeed, it is widely known that the intrarenal renin-angiotensin system is highly active, especially in the renal tubules (2). However, in mesangial cells, there are only a few reports on the activation of local renin-angiotensin system, and the existence of mechanical strain-induced local Ang II formation has not been reported. In the present study, evidence of a local activation of the renin-angiotensin system is not observed, but the effect seems to be mediated by AT1R because the knockdown of $AT_{1A}R$ using miRNA has the same effect as olmesartan. These observations indicate that cyclic mechanical strain stimulates AT1R independent of Ang II.

A recent study reported AT1R activation by mechanical strain in the absence of Ang II in cardiomyocytes, leading to the activation of JNK, p38 MAPK, and ERK (29). Endogenous activation of renin-angiotensin system is also not detected in strain-exposed cardiomyocytes since the cells were obtained from angiotensinogen-null mice. Our present report demonstrates that a similar signal transduction system may exist in renal mesangial cells. However, the findings more closely resemble the physiological situation because in the present study the cells were isolated from normal Sprague-Dawley rats with an intact renin-angiotensin system. There are also differences between the reported studies in cardiac myocytes and our studies in renal mesangial cells. In cardiac myocytes, the

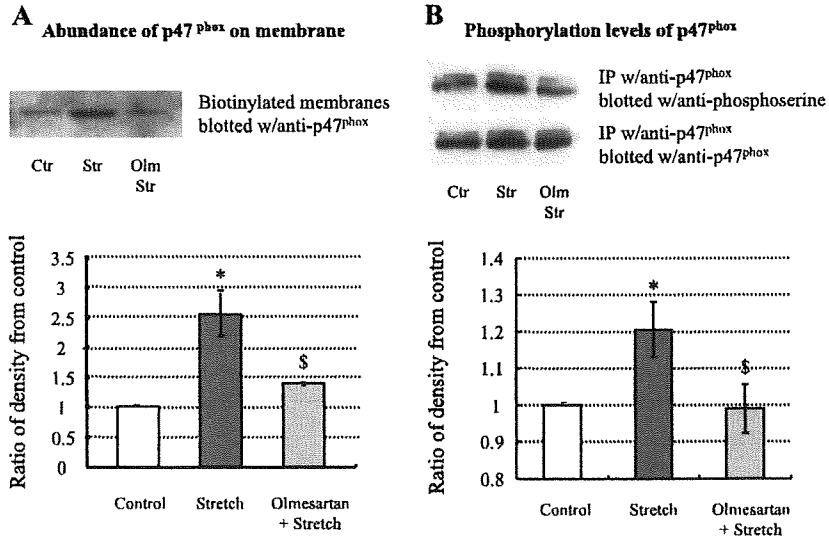

Fig. 5. Olmesartan attenuates the membrane translocation and phosphorylation of p47^{phox} by stretch (Str). Abundance of p47^{phox} on cell surface membranes (*A*) and phosphorylation levels of p47^{phox} (*B*) are shown. Olmesartan (10^{-5} M) significantly decreased membrane translocation and phosphorylation of p47^{phox}. Means ± SE (n = 4) are given. $*P < 0.05$ vs. control; $\$P < 0.05$ vs. stretch group. IP, immunoprecipitate.

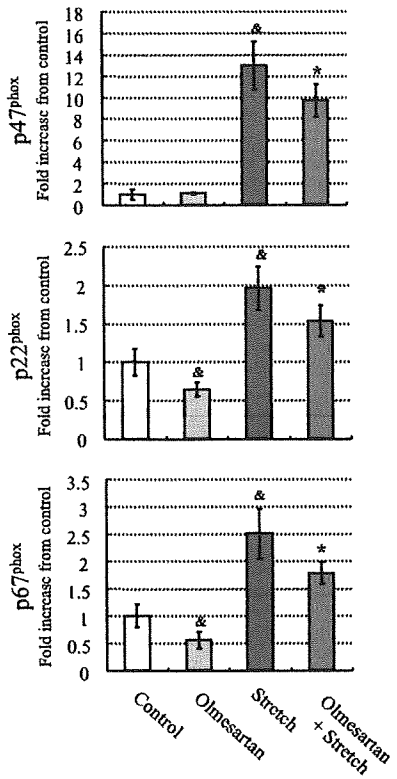

Fig. 6. Changes in the mRNA expression levels of NADPH oxidase subunits $p47^{phox}$, $p22^{phox}$, and $p67^{phox}$. Quantification of mRNA was determined on the basis of the C_t value, normalized to β-actin, and expressed as the magnitude of change under mechanical strain application relative to the corresponding control. Means ± SE (n = 3) are given. &$P < 0.01$ vs. control; *$P < 0.01$ vs. stretch group.

maximal inhibition of ERK phosphorylation with AT1R blockade is observed at the initial peak after 8 min in cardiomyocytes, as opposed to the plateau phase after 60 min of stretch stress in mesangial cells. There are several cell signaling molecules that activate ERK, such as integrins (10, 15) and intracellular calcium ion accumulation (10). In additional studies, early-phase activation of ERK induced by cyclic mechanical strain is abolished by preincubation with either cytochalasin D, a potent inhibitor of actin polymerization, or BAPTA-TM, a calcium ion chelator. However, these treatments minimally affect the phosphorylation levels of ERK at the plateau phase (Fig. 7). It is possible that the initial peak of ERK phosphorylation with mechanical strain is caused mainly by the early signal transduction systems (e.g., calcium influx or cytoskeleton modification), such that the effect of AT1R may be masked by these short-term signals but becomes apparent only at the plateau phase. Since stretch stress attributable to high blood pressure is a chronic stimulus, the effects of AT1R activation and antagonism at the plateau phase may be more relevant in the pathogenesis of long-term organ damage.

We found that Tempol, a potent superoxide dismutase mimetic, decreases the phosphorylation levels of ERK at the plateau phase. To evaluate further the mechanisms of ERK activation caused by strain through AT1R at the plateau phase, the role of NADPH oxidase activation, one of the major sources of O_2^- and H_2O_2 in oxidative stress, was evaluated. Previous studies have shown that Ang II activates NADPH oxidase (5, 11, 14), and the resulting oxidative stress in turn activates the MAPK cascade (3, 7). In the present study, we show that mechanical strain increases both the translocation of $p47^{phox}$ to the cell membrane and phosphorylated levels of $p47^{phox}$, which may reflect NADPH oxidase activation (25). As stated earlier, calcium ion influx leads to rapid activation of ERK, whereas the activation of ERK through H_2O_2 production via NADPH oxidase activation may take longer (26). This is indeed the case; H_2O_2 increases phospho-ERK gradually with the highest value observed at 60 min. The activation of NADPH oxidase and production of reactive oxygen species may explain the delayed effect of AT1R blockade on ERK activation induced by mechanical strain. However, there have been reports that ARBs, including olmesartan, are potent antioxidants (11). It is possible that part of the attenuation of mechanical strain-induced ERK phosphorylation may be exerted through the free-radical scavenging of olmesartan in combination with the Ang II-independent AT1R inactivation.

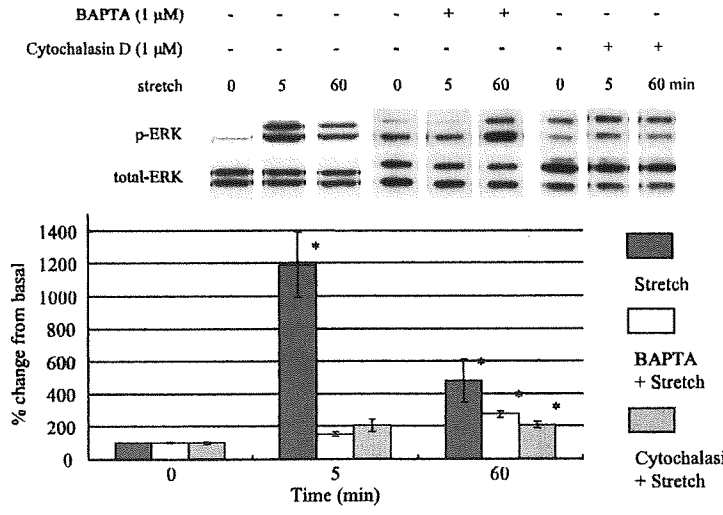

Fig. 7. Effect of BAPTA and cytochalasin D on stretch-induced ERK phosphorylation. Phosphorylation levels of ERK were expressed as % change from control. The early-phase (5 min) activation of ERK induced by cyclic mechanical strain was abolished almost completely by preincubation with either 1 μM of BAPTA-TM or 1 μM of cytochalasin D. In contrast, the phosphorylation of ERK at the plateau phase (60 min) by mechanical strain was still observed with BAPTA-TM or cytochalasin D (BAPTA-TM; 273.7 ± 20.5%, cytochalasin D; 208.5 ± 19.8% compared with no stretch control). Means ± SE (n = 4) are given. *$P < 0.01$ vs. control.

Olmesartan has a greater blood pressure-lowering and organ-protective effects than other ARBs (23, 24). Some investigators speculate that these enhanced effects may be related to the inverse agonistic activity of ARBs. Some receptor antagonists have inhibitory effects in spite of the absence of specific agonists; these drugs are called inverse agonists (17, 29). Olmesartan has strong inverse agonist activity against constitutively active AT1-F77A or N111G mutant AT1R, relative to losartan (18, 19). Indeed, losartan has been reported to prevent Ang II-induced, but not stretch-induced, VEGF protein secretion in human mesangial cells (8). In the present study, olmesartan but not losartan significantly attenuates stretch-induced, agonist-independent ERK activation in mesangial cells. This observation can be explained by the strong inverse-agonist effect of olmesartan (18, 19). Olmesartan, unlike losartan, has α-carboxyl groups, and of the currently available ARBs olmesartan has the largest number of estimated binding domains that can interact with AT1R. The greater number of interacting domains and affinity to AT1R possibly affect the potency of inverse agonistic activity of ARBs. Olmesartan also significantly decreases basal and stretch-induced NADPH oxidase subunit mRNA expression. Our results show that there may be a low level of constitutive AT1R activity in cultured RMCs, which can be blocked by a potent inverse agonist of AT1R such as olmesartan. Another inverse agonist of AT1R, candesartan, was also able to attenuate the agonist-independent, stretch-induced AT1R activation in cardiomyocytes (29). In that report, a competitive inhibitor for Ang II, (Sar1, Ile8)-Ang II, was unable to replicate the effect of candesartan. Further investigation will be required to determine whether other ARBs with inverse-agonist effect can also block Ang II-independent, stretch-induced AT1R activation.

We have recently demonstrated that selective knockdown of renal AT1R expression using antisense oligodeoxynucleotides markedly reduces urinary protein excretion and glomerular sclerosis in spontaneously hypertensive rats (28). The reduction in urinary protein excretion and glomerular sclerosis occurs despite elevated circulating Ang II and aldosterone levels and sustained high blood pressure. This may be due to the fact that both Ang II-dependent and Ang II-independent mechanical stretch-induced AT1R activation are blocked by the knockdown of the AT1R gene. Although a high salt intake decreases plasma renin activity and aldosterone in hypertensive patients (6, 16), renal damage is not prevented. It is possible that the hypertensive renal damage and mesangial proliferation in these patients may partly be caused by agonist-independent, stretch stress-induced AT1R activation.

In conclusion, cyclic mechanical strain increases the phosphorylation levels of ERK and activates NADPH oxidase in mesangial cells in the absence of local Ang II production. These effects are blocked by olmesartan, an ARB with inverse agonistic activity. The ARBs with inverse agonistic activity such as olmesartan could be beneficial in the prevention of renal mesangial proliferation and hypertensive organ damage regardless of circulating or tissue Ang II levels.

ACKNOWLEDGMENTS

The authors thank Hiroko Ohashi for technical assistance. Olmesartan was kindly supplied by Daiichi-Sankyo Pharmaceutical Co., Ltd. (Tokyo, Japan).

GRANTS

This work was supported in part by the Fukushima Society for the Promotion of Medicine (No. 18) and Salt Science Foundation (No. 0835).

REFERENCES

1. **Ardaillou R, Chansel D, Chatziantoniou C, Dussaule JC.** Mesangial AT1 receptors: expression, signaling, and regulation. *J Am Soc Nephrol* 10, *Suppl* 11: S40–S46, 1999.
2. **Bader M, Peters J, Baltatu O, Muller DN, Luft FC, Ganten D.** Tissue renin-angiotensin systems: new insights from experimental animal models in hypertension research. *J Mol Med* 79: 76–102, 2001.
3. **Brandes RP, Kreuzer J.** Vascular NADPH oxidases: molecular mechanisms of activation. *Cardiovasc Res* 65: 16–27, 2005.
4. **Cai H, Griendling KK, Harrison DG.** The vascular NAD(P)H oxidases as therapeutic targets in cardiovascular diseases. *Trends Pharmacol Sci* 24: 471–478, 2003.
5. **Chabrashvili T, Kitiyakara C, Blau J, Karber A, Aslam S, Welch WJ, Wilcox CS.** Effects of ANG II type 1 and 2 receptors on oxidative stress, renal NADPH oxidase, and SOD expression. *Am J Physiol Regul Integr Comp Physiol* 285: R117–R124, 2003.
6. **de la Sierra A, Lluch MM, Coca A, Aguilera MT, Giner V, Bragulat E, Urbano-Marquez A.** Fluid, ionic and hormonal changes induced by high salt intake in salt-sensitive and salt-resistant hypertensive patients. *Clin Sci (Lond)* 91: 155–161, 1996.
7. **Gorin Y, Ricono JM, Wagner B, Kim NH, Bhandari B, Choudhury GG, Abboud HE.** Angiotensin II-induced ERK1/ERK2 activation and protein synthesis are redox-dependent in glomerular mesangial cells. *Biochem J* 381: 231–239, 2004.
8. **Gruden G, Thomas S, Burt D, Zhou W, Chusney G, Gnudi L, Viberti G.** Interaction of angiotensin II and mechanical stretch on vascular endothelial growth factor production by human mesangial cells. *J Am Soc Nephrol* 10: 730–737, 1999.
9. **Hori Y, Katoh T, Hirakata M, Joki N, Kaname S, Fukagawa M, Okuda T, Ohashi H, Fujita T, Miyazono K, Kurokawa K.** Anti-latent TGF-beta binding protein-1 antibody or synthetic oligopeptides inhibit extracellular matrix expression induced by stretch in cultured rat mesangial cells. *Kidney Int* 53: 1616–1625, 1998.
10. **Iqbal J, Zaidi M.** Molecular regulation of mechanotransduction. *Biochem Biophys Res Commun* 328: 751–755, 2005.
11. **Izuhara Y, Nangaku M, Inagi R, Tominaga N, Aizawa T, Kurokawa K, van Ypersele de Strihou C, Miyata T.** Renoprotective properties of angiotensin receptor blockers beyond blood pressure lowering. *J Am Soc Nephrol* 16: 3631–3641, 2005.
12. **Kitiyakara C, Chabrashvili T, Chen Y, Blau J, Karber A, Aslam S, Welch WJ, Wilcox CS.** Salt intake, oxidative stress, and renal expression of NADPH oxidase and superoxide dismutase. *J Am Soc Nephrol* 14: 2775–2782, 2003.
13. **Lee MA, Bohm M, Paul M, Ganten D.** Tissue renin-angiotensin systems. Their role in cardiovascular disease. *Circulation* 87: IV7–IV13, 1993.
14. **Li JM, Shah AM.** Mechanism of endothelial cell NADPH oxidase activation by angiotensin II. Role of the p47phox subunit. *J Biol Chem* 278: 12094–12100, 2003.
15. **MacKenna DA, Dolfi F, Vuori K, Ruoslahti E.** Extracellular signal-regulated kinase and c-Jun NH2-terminal kinase activation by mechanical stretch is integrin-dependent and matrix-specific in rat cardiac fibroblasts. *J Clin Invest* 101: 301–310, 1998.
16. **McKnight JA, Roberts G, Sheridan B, Atkinson AB.** The effect of low and high sodium diets on plasma atrial natriuretic factor, the renin-aldosterone system and blood pressure in subjects with essential hypertension. *Clin Endocrinol (Oxf)* 40: 73–77, 1994.
17. **Milligan G.** Constitutive activity and inverse agonists of G protein-coupled receptors: a current perspective. *Mol Pharmacol* 64: 1271–1276, 2003.
18. **Miura S, Kiya Y, Kanazawa T, Imaizumi S, Fujino M, Matsuo Y, Karnik SS, Saku K.** Differential bonding interactions of inverse agonists of angiotensin II type 1 receptor in stabilizing the inactive state. *Mol Endocrinol* 22: 139–146, 2008.
19. **Miura S, Fujino M, Hanzawa H, Kiya Y, Imaizumi S, Matsuo Y, Tomita S, Uehara Y, Karnik SS, Yanagisawa H, Koike H, Komuro I, Saku K.** Molecular mechanism underlying inverse agonist of angiotensin II type 1 receptor. *J Biol Chem* 281: 19288–19295, 2006.

20. **Navar LG, Harrison-Bernard LM, Imig JD, Wang CT, Cervenka L, Mitchell KD.** Intrarenal angiotensin II generation and renal effects of AT1 receptor blockade. *J Am Soc Nephrol* 10, *Suppl* 12: S266–S272, 1999.
21. **Navar LG, Inscho EW, Majid SA, Imig JD, Harrison-Bernard LM, Mitchell KD.** Paracrine regulation of the renal microcirculation. *Physiol Rev* 76: 425–536, 1996.
22. **Onozaki A, Midorikawa S, Sanada H, Hayashi Y, Baba T, Katoh T, Watanabe T.** Rapid change of glucose concentration promotes mesangial cell proliferation via VEGF: inhibitory effects of thiazolidinedione. *Biochem Biophys Res Commun* 317: 24–29, 2004.
23. **Oparil S, Williams D, Chrysant SG, Marbury TC, Neutel J.** Comparative efficacy of olmesartan, losartan, valsartan, and irbesartan in the control of essential hypertension. *J Clin Hypertens (Greenwich)* 3: 283–291; 318, 2001.
24. **Sanada S, Kitakaze M, Node K, Takashima S, Ogai A, Asanuma H, Sakata Y, Asakura M, Ogita H, Liao Y, Fukushima T, Yamada J, Minamino T, Kuzuya T, Hori M.** Differential subcellular actions of ACE inhibitors and AT(1) receptor antagonists on cardiac remodeling induced by chronic inhibition of NO synthesis in rats. *Hypertension* 38: 404–411, 2001.
25. **Touyz RM, Yao G, Schiffrin EL.** c-Src induces phosphorylation and translocation of p47phox: role in superoxide generation by angiotensin II in human vascular smooth muscle cells. *Arterioscler Thromb Vasc Biol* 23: 981–987, 2003.
26. **Touyz RM, Yao G, Viel E, Amiri F, Schiffrin EL.** Angiotensin II and endothelin-1 regulate MAP kinases through different redox-dependent mechanisms in human vascular smooth muscle cells. *J Hypertens* 22: 1141–1149, 2004.
27. **van Biesen T, Luttrell LM, Hawes BE, Lefkowitz RJ.** Mitogenic signaling via G protein-coupled receptors. *Endocr Rev* 17: 698–714, 1996.
28. **Yoneda M, Sanada H, Yatabe J, Midorikawa S, Hashimoto S, Sasaki M, Katoh T, Watanabe T, Andrews PM, Jose PA, Felder RA.** Differential effects of angiotensin II type-1 receptor antisense oligonucleotides on renal function in spontaneously hypertensive rats. *Hypertension* 46: 58–65, 2005.
29. **Zou Y, Akazawa H, Qin Y, Sano M, Takano H, Minamino T, Makita N, Iwanaga K, Zhu W, Kudoh S, Toko H, Tamura K, Kihara M, Nagai T, Fukamizu A, Umemura S, Iiri T, Fujita T, Komuro I.** Mechanical stress activates angiotensin II type 1 receptor without the involvement of angiotensin II. *Nat Cell Biol* 6: 499–506, 2004.

Clin Exp Nephrol (2010) 14:56–62
DOI 10.1007/s10157-009-0243-x

ORIGINAL ARTICLE

Genetical, histological, and clinical characteristics of IgA-negative mesangioproliferative glomerulopathy

Kazunori Owada · Hodaka Suzuki · Tetsuo Katoh · Tsuyoshi Watanabe

Received: 25 May 2009 / Accepted: 8 October 2009 / Published online: 25 November 2009

Abstract
Background Mesangioproliferative glomerulopathy (MesPGN) is a well-defined pathohistological entity. However, the clinical characteristics and prognosis have not been fully established in patients without immunoglobulin (Ig)A (N-IgAN) in contrast to patients with IgA nephropathy (IgAN).
Methods A total of 837 consecutive patients underwent renal biopsies. Among them, 465 patients were diagnosed with MesPGN by light microscopy. With immunofluorescent study and electron microscopy (EM), 344 were diagnosed as having IgAN. Among the rest, 84 patients who had no immunofluorescence evidence of IgA and no deposits in EM were defined as N-IgAN. We compared the clinical characteristics, histological findings, and genotypes of the angiotensin-converting enzyme (ACE) gene and plasminogen activator inhibitor-1 gene between IgAN and N-IgAN patients.
Results Urinary protein excretion and the degree of hematuria were significantly lower in N-IgAN than IgAN patients (0.50 vs. 0.82 g/day; $P = 0.01$), (1.33 vs. 2.50; $P < 0.001$, respectively). Creatinine clearance was higher in N-IgAN than IgAN patients (89.4 vs. 74.4 ml/min; $P < 0.001$). Histopathologically, N-IgAN patients had significantly less advanced glomerular and tubulointerstitial lesions than IgAN patients. Pathological grades in patients with untreated IgAN were more advanced in a time-dependent manner, whereas there was no relationship between histological grades and time of illness in N-IgAN patients. Frequency of the DD genotype of the ACE gene was significantly lower in N-IgAN (DD/ID+II = 8/76) than IgAN (24/90) patients.
Conclusions IgA-negative MesPGN is a distinct type of glomerulopathy with a benign renal prognosis. Insertion/deletion polymorphisms of the ACE gene may play some role in the genesis and progression of MesPGN.

Keywords ACE polymorphism · IgA nephropathy · Mesangioproliferative glomerulopathy

K. Owada · H. Suzuki · T. Katoh (✉) · T. Watanabe
Department of Internal Medicine III, Fukushima Medical University School of Medicine, 1 Hikarigaoka, Fukushima 960-1295, Japan
e-mail: t-katoh@fmu.ac.jp

Introduction

Mesangioproliferative glomerulopathy (MesPGN) is a well-defined pathohistological entity with increased cell number and extracellular matrix in the glomerular mesangium [1–3]. Patients with immunodeposits containing immunoglobulin (Ig)A in the mesangium are denoted as having IgA nephropathy (IgAN), which is recognized as the most common form of primary glomerulopathy worldwide, particularly in southern Europe and eastern Asia. IgAN is a heterogeneous disease, with 30–40% of IgAN patients developing end-stage renal disease (ESRD) in a 20-year observation period [3–5]. In contrast, for patients with MesPGN and without IgA deposition (N-IgAN), there are few reports describing its clinical characteristics and prognosis [1]. It is still uncertain whether it may be a unique disease entity or whether it is a histological "trash box" for diverse pathologic conditions, with only clinically present asymptomatic proteinuria and/or hematuria.

It has been suggested that genetic factors may influence the pathogenesis and prognosis of renal glomerular

diseases [6–12]. Insertion/deletion (I/D) polymorphisms of angiotensin-converting enzymes (ACE) have been demonstrated to be significantly associated with the incidence and prognosis of various cardiovascular disorders [13–15] and progression of glomerular disease. An I/D polymorphism of the ACE gene plays an important role in the progression of IgAN [9–11]; however, its exact role is still controversial [16–19]. It also remains to be elucidated whether I/D polymorphisms of the ACE gene may affect the pathogenesis and progression of N-IgAN. We previously reported that the 4G/5G polymorphism of the plasminogen activator inhibitor-1 (PAI-1) gene is associated with IgAN progression [12], whereas its role in N-IgAN has not been reported. In this study, we investigated the clinical characteristics, renal pathological findings, and genotypes of the ACE and PAI-1 genes patients with N-IgAN in comparison with those with IgAN.

Methods

Patients and definition of non-IgA glomerulopathy (N-IgAN)

Renal biopsies were performed at the Third Department of Medicine, Fukushima Medical University, for patients with proteinuria ≥2+ by dipstick urine test or with both proteinuria (≥1+) and hematuria or with hematuria (≥1+) for more than 1 year without urological abnormalities. We defined MesPGN as being four or more cells per mesangial area. At least 80% of glomeruli should be involved [20, 21], with a mesangial matrix index (MMI) >7% of glomeruli. We regard an MMI of <7% as minor glomerular abnormality and distinguished such cases from N-IgAN. Among 961 consecutive renal biopsy specimens acquired between January 1999 and October 2005, 465 patients were diagnosed with mesangioproliferative glomerulitis by light microscopy according to the criteria. Based on immunofluorescent and electron microscopy (EM) analyses, 344 of these patients were diagnosed with IgAN and 23 with purpura nephritis. In addition, 84 patients whose specimens showed no IgA under immunofluorescence examination and no dense deposits detected by EM were diagnosed with N-IgAN [1–3]. A total of 14 patients whose specimens showed dense deposits by EM but not upon immunofluorescence were excluded from the study. Of the 344 IgAN patients, 114 patients who were consecutively diagnosed with N-IgAN through January 1999 to December 2000 were examined to make the number of each group comparable.

The grade of microscopic hematuria was defined with a high power field (HPF) and was rated as 0 [1–4 red blood cells (RBC)/HPF), 1 (5–9 RBC/HPF), 2 (10–29 RBC/HPF), 3 (30–50 RBC/HPF), 4 (50–100 RBC/HPF), or 5 (>100 RBC/HPF). Blood pressure level was defined as the mean level of three consecutive measurements on different days during admission at our hospital. Mean urinary protein excretion was determined for 3 days.

Genetic analysis of ACE polymorphism

DNA was isolated from peripheral blood leukocytes using a commercial kit (BDtract™, Maxim Biotech, Inc., USA) and was used for polymerase chain reaction (PCR). Two primers were designed to flank the polymorphic region of the ACE gene. The sense oligonucleotide primer was 5′-CTGGAGACCACTCCCATCCTTTCT-3′ and the antisense primer was 5′-GATGTGGCCATCACATTCGAC AGAT-3′. For the amplification reaction, 80 ng genomic DNA was used in a final volume 50 μl containing 3 mM magnesium chloride ($MgCl_2$), 50 mM potassium chloride (KCl), 10 mM Tris–HCl (pH 8.4), 10 pmol of each primer, 0.2 mM of each deoxynucleotide triphosphate (dNTP), and 1 U Taq polymerase (Takara, Tokyo, Japan). DNA was amplified using a DNA thermal cycler (Takara, Tokyo, Japan) with 1-min denaturation at 94°C, 1-min annealing at 55°C, and 2-min extension at 72°C for 30 cycles. In the last cycle, the extension step was carried out for 10 min. PRC products were separated on 1.5% agarose gels and visualized by ethidium bromide staining.

Genetic analysis of PAI-1 4G/5G polymorphism

We also analyzed the genotype of the 4G/5G polymorphism with a method combining rapid-cycle PCR with real-time monitoring of the amplification process and the generation of allele-specific fluorescent probe melting profiles on a LightCycler™ (Roche, Basel, Switzerland) [22]. The primers 5′-AGCCAGACAAGGTTGTTGACA C-3′ and 5′-CAGAGGACTCTTGGTCTTTCCC-3′ were used to amplify, respectively, a 134- or 135-bp fragment of the PAI-1 gene (GenBank accession no. X13323). The detection probe was an 18-mer oligonucleotide labeled at the 3′-end with fluorescein. The sequence 5′-TGACT CCCCCACGTGTCCT-3′ is complementary to the leading strand of the 5G allele. The anchor probe (5′-AC TCTCTCTGTGCCCCTGAGGGCTCT-3′) was a 26-mer labeled with LightCycler Red 640 at its 5′-end and modified at the 3′-end by phosphorylation to block extension. PCR was performed by rapid cycling in a reaction volume of 10 μl with 0.3 μM of each primer, 0.2-μM anchor and detection probes, and 50 ng genomic DNA. After an initial denaturation step at 94°C for 45 s, amplification was performed using 50 cycles of denaturation (94°C for 0 s), annealing (57°C for 5 s), and extension (72°C for 2 s).

Histopathological analysis

Lesions detected by light microscopy in MesPGN patients were classified into four glomerular grades and three tubulointerstitial grades described below.

G0: Glomerulosclerosis, crescent formation, or adhesion to Bowman's capsule is not observed.

G1: Glomerulosclerosis, crescent formation, or adhesion to Bowman's capsule seen in <10% of all biopsied glomeruli.

G2: Glomerulosclerosis, crescent formation, or adhesion to Bowman's capsule seen in 10–30% of all biopsied glomeruli.

G3: Glomerulosclerosis, crescent formation, or adhesion to Bowman's capsule seen in >30% of all biopsied glomeruli. When sites of sclerosis are totaled and converted to global sclerosis, the sclerosis rate is >50% of all glomeruli. Some glomeruli also show compensatory hypertrophy.

T1: Prominent changes are not seen in the interstitium, renal tubuli, or blood vessels.

T2: Cellular infiltration is slight in the interstitium except around some sclerosed glomeruli. Tubular atrophy is slight, and mild vascular sclerosis is observed.

T3: Interstitial cellular infiltration and tubular atrophy, as well as fibrosis, are seen. Hyperplasia or degeneration is seen in some intrarenal arteriolar walls.

The degree of glomerular matrix accumulation was examined by imaging analysis consisting of the following steps, as described previously [23]: (1) capturing glomeruli on the periodic acid Schiff (PAS) preparation at a magnitude of 200×, (2) tracing the outline of the glomeruli to obtain the whole glomerular area, (3) selecting the PAS-positive area manually with the mouse pointer. Finally, MMI was calculated from the ratio of the PAS-positive area to glomerular area measured as above. The mean of each glomerular MMI in the specimens was regarded as representing the magnitude of matrix accumulation in each case. Control values of MMI were obtained from needle biopsy specimens from patients with minimal-change nephrotic syndrome (MCD) ($n = 39$).

All renal biopsy samples were examined independently by a researcher who was not provided with any clinical information about the patients. The study was approved by the research ethics committee at Fukushima Medical University.

Statistical analysis

All data are presented as mean ± standard deviation (SD). As nonnormal distributions or inequality of variances was present in some variables, nonparametric analysis was performed. Statistical comparisons were performed using Mann–Whitney's U test and chi-square test for independence. Values of $P < 0.05$ were regarded as statistically significant. These calculations were performed with StatView, Ver. 5.0 (Abacus Concepts, Berkeley, CA, USA).

Results

Clinical characteristics of patients with N-IgAN and those with IgAN are shown in Table 1. Urinary protein excretion (0.50 ± 0.66 vs. 0.82 ± 1.26 g/day; $P = 0.01$, respectively) and degree of hematuria (1.33 ± 1.60 vs. 2.50 ± 1.57; $P < 0.001$, respectively) were significantly lower in patients with N-IgAN than in those with IgAN. Creatinine clearance (Ccr) was higher in N-IgAN in IgAN patients (89.4 ± 29.7 vs. 74.4 ± 25.1 ml/min; $P = 0.001$, respectively). Serum concentration of IgA was lower in N-IgAN than IgAN patients (236 ± 107 vs. 404 ± 157 mg/dl; $P < 0.001$, respectively). Age at the time of renal biopsy (40.92 ± 16.00 vs. 36.67 ± 14.94 years old, respectively), gender (male/female 50/34 vs. 59/55, respectively), duration of hematuria and/or proteinuria (7.38 ± 7.86 vs. 7.13 ± 7.58 years, respectively), serum creatinine (0.89 ± 0.32 vs. 1.01 ± 0.58 mg/dl, respectively), and systolic blood pressure (128.02 ± 17.59 vs. 123.42 ± 15.30 mmHg, respectively) did not differ.

The degree of mesangial matrix accumulation measured by MMI was increased by rank of order as in patients with IgAN, N-IgAN, and controls (MCD group) (13.65 ± 5.01, 9.83 ± 3.37, and 3.99 ± 1.57%, respectively $P < 0.001$) (Fig. 1). As shown in Fig. 2a and b, glomerular and tubulointerstitial changes were significantly milder in N-IgAN than IgAN patients (G0, G1, G2, and G3 were 33, 28, 14, and 9; and 18, 20, 44, and 32, respectively; T1, T2, and T3 were 58, 14, and 12; and 39, 46, and 29, respectively), as estimated by chi-square test. There were no obvious differences in vascular changes, although we did no quantitative evaluation.

To examine the time dependency of histological findings, glomerular and tubulointerstitial grades as well as other clinical characteristics in patients with ≥6 years between onset of proteinuria and renal biopsy (longer duration) were compared with those with an interval <6 years (shorter duration) (Tables 2 and 3). IgAN of shorter duration had significantly milder glomerular findings (G0:G1:G2:G3 14:15:25:14 vs. 4:5:19:18, respectively, $P = 0.043$) (Table 2, and Fig. 3a), and creatinine was lower (0.95 ± 0.50 vs. 1.11 ± 0.66 mg/dl, respectively; $P = 0.0188$) and higher (80.53 ± 23.48 vs. 65.31 ± 24.58 ml/min, respectively; $P = 0.0008$) (Table 2). Disease duration did not affect tubulointerstitial findings in

Table 1 Clinical characteristics of patients with mesangioproliferative glomerulopathy without immunoglobulin (Ig)A deposition (N-IgAN) and with IgA nephropathy (IgAN)

	N-IgAN (n = 84)	IgAN (n = 114)	P value
Age (year)	40.92 ± 16.00	36.67 ± 14.94	0.48
Male:female	50:34	59:55	0.35
Interval from the onset (year)	7.38 ± 7.86	7.13 ± 7.58	0.93
BP (S) mmHg	128.02 ± 17.59	123.42 ± 15.30	0.10
BP (D) mmHg	76.45 ± 11.92	73.55 ± 11.45	0.02
Urinary protein excretion (g/day)	0.50 ± 0.66	0.821 ± 1.26	0.01
Hematuria score	1.33 ± 1.60	2.50 ± 1.57	<0.001
Crea (mg/dl)	0.89 ± 0.32	1.01 ± 0.58	0.07
Ccr (ml/min)	89.35 ± 29.74	74.39 ± 25.08	0.01
IgA (mg/dl)	236 ± 107	404 ± 157	<0.001
G grade (G0:G1:G2:G3)	33:28:14:9	18:20:44:32	<0.001
G grade score	0.99 ± 1.00	1.78 ± 1.03	<0.001
T grade (T1:T2:T3)	58:14:12	39:46:29	<0.001
T grade score	1.45 ± 0.74	1.87 ± 0.64	<0.001
MMI (%)	9.83 ± 3.37	13.65 ± 5.01	<0.001
ACE polymorphism (DD:ID:II)	8:41:35	24:48:42	0.03
PAI-1 polymorphism (4G4G:4G5G:5G5G)	15:36:9	40:54:20	0.38

Serum creatinine in mg/dl may be converted to μmol/l by multiplying by 88.4

BP (S) systolic blood pressure, *BP (D)* diastolic blood pressure, *Crea* creatinine, *Ccr* creatinine clearance, *MMI* mesangial matrix index, *ACE* angiotensin-converting enzyme, *PAI-1* plasminogen activator inhibitor-1

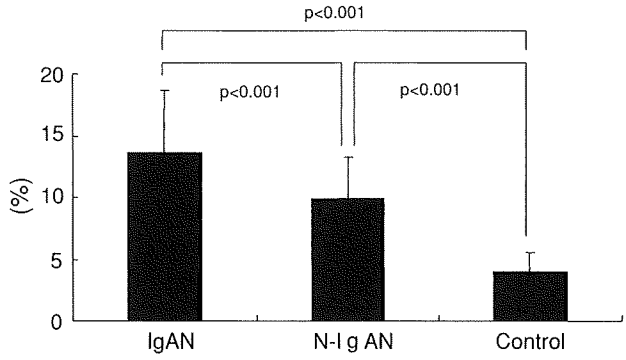

Fig. 1 Degree of mesangial matrix accumulation measured by mesangial matrix index (*MMI*) is significantly increased in patients with immunoglobulin (Ig)A nephropathy (*IgAN*) compared with patients with mesangioproliferative glomerulopathy without IgA deposition (*N-IgAN*). MMI in N-IgAN patients is significantly increased compared with the control group

either group (T1:T2:T3 24:35:9 in shorter duration vs. 8:31:7 in longer duration, respectively, $P = 0.11$) (Table 2). On the other hand, in patients with N-IgAN, there was no difference in the histopathology between those with shorter duration and longer duration (G0:G1:G2:G3 23:11:7:4 vs. 10:17:7:5, respectively, and T1:T2:T3 33:7:5 vs. 25:7:7, respectively) (Table 3; Fig. 3b), suggesting a less progressive nature of N-IgAN compared with IgAN.

Figure 4a demonstrates that the frequency of the DD genotype was significantly lower in patients with N-IgAN (DD:ID+II 8:76) than those with IgAN (DD:ID+II 24:90, $P = 0.0294$) or healthy control volunteers (DD:ID+II 53:217, $P = 0.033$), whereas the PAI-1 gene allele frequency of 4G4G was similar in N-IgAN and IgAN patients and healthy control volunteers (Fig. 4b).

Patients with N-IgAN were followed up for 3.25 ± 1.91 (range 0.8–7) years, having taken essentially no medications. Their renal function did not deteriorate (from 0.89 ± 0.32 to 0.93 ± 0.71 mg/dl, $P = 0.073$), whereas those with IgAN decreased from 1.01 ± 0.58 to 1.17 ± 0.69 mg/dl, $P = 0.134$) with treatment by steroid, ACE-inhibitor, and/or angiotensin receptor blocker (ARB). Data indicate that there were few changes in renal function in patients with N-IgAN without any specific treatment.

Discussion

Mesangioproliferative glomerulonephritis is the most common form of primary glomerulopathies. Among them, IgAN is the most common and well-characterized. In contrast, the clinical course and pathophysiology of N-IgAN has not been well described. This study demonstrated that MesPGN without IgA deposition might take a benign course compared with MesPGN with IgAN (Tables 2, 3; Figs. 2a, b, 3a, b). The clinical and histological characteristics were significantly and clearly different between patients with IgAN and those with N-IgAN (Table 1; Fig. 2a, b), suggesting that the basic pathological processes in N-IgAN are independent of those of IgAN.

In the genotyping assay, the low frequency of the DD genotype in patients wtih N-IgAN may indicate that the pathogenesis of N-IgAN is distinguished from IgAN (Fig. 4a). The genotype of ACE in IgAN patients as well

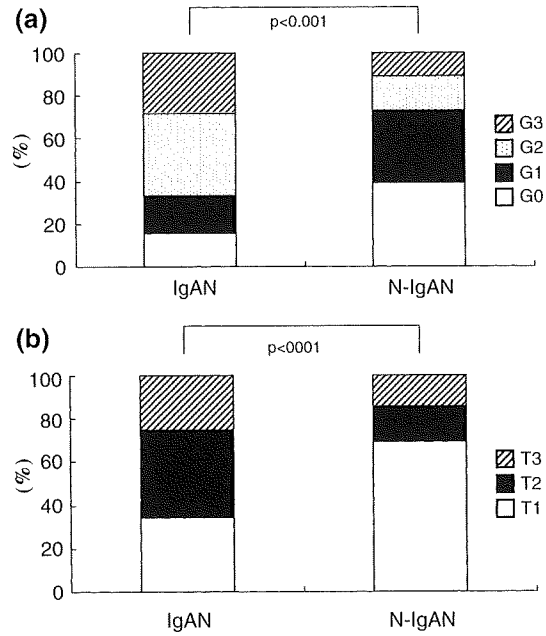

Fig. 2 **a** Degree of pathological glomerular changes are significantly milder in patients with mesangioproliferative glomerulopathy without immunoglobulin (Ig)A deposition (*N-IgAN*) than those with IgA nephropathy (*IgAN*) by chi-square test. As indicated, the ratio of G0+G1 is 72.6% in N-IgAN patients and 33.3% in those with IgAN. **b** Degree of pathological tubulointerstitial changes are significantly milder in patients with mesangioproliferative glomerulopathy without IgA deposition (*N-IgAN*) than those with IgA nephropathy (*IgAN*) by chi-square test. As indicated, the ratio of T1 is 69.0% in N-IgAN patients and 34.2% in IgAN patients

as normal controls, of which samples were examined in parallel with those of patients with N-IgAN, were similar with the average frequency in the Japanese population [9, 24, 25], which indicates that technical bias was unlikely. Moreover, the genotypes of PAI-1, which we previously demonstrated [12] to be associated with the progression of histological changes and a decrease in kidney function, are similar in N-IgAN and IgAN patients, thus suggesting a unique genotypic feature of ACE in N-IgAN patients. The sample size of N-IgAN patients was adequate for statistical analysis of gene polymorphisms of ACE, also considering its distribution in the Japanese population.

Patients with the DD genotype are supposed to have higher local angiotensin II concentrations, and angiotensin II promotes pathological glomerular processes [26]. The small number of DD genotypes in N-IgAN patients may indicate that N-IgAN is a less advanced subgroup of this particular disorder. It could be speculated that N-IgAN is a less pathogenic subtype of IgAN, because angiotensin II has been demonstrated to stimulate mesangial uptake of immune complexes, possibly resulting in IgA accumulation in mesangial cells [27]. However, the frequency of the DD genotype in IgAN patients was not increased compared with the control population in this study, a result reported by others [16, 18]. The influence of the low frequency of the DD genotype in N-IgAN patients should be further investigated.

In conclusion, these findings suggest that N-IgAN is a distinct type of primary glomerular disorder and is clearly distinguished from IgAN by clinical, histological and genetic characteristics, although there should be several limitations because of the relatively small number of patients in this study. The I/D polymorphism of the ACE gene may play some role in the genesis and progression of MesPGN.

Table 2 Comparison of clinical characteristics in patients with ≥6 years between onset of proteinuria and renal biopsy and in those with an interval of <6 years in immunoglobulin (IgA) nephropathy (IgAN)

IgAN	<6 years (n = 68)	≥6 years (n = 46)	P value
Age (year)	35.25 ± 14.99	45.15 ± 13.63	<0.001
Male:female	35:33	24:22	0.9
Interval from onset (year)	2.07 ± 1.55	14.33 ± 6.85	<0.001
BP (S) mmHg	121.68 ± 15.06	126.84 ± 16.33	0.13
BP (D) mmHg	71.52 ± 10.63	76.94 ± 12.19	0.02
Urinary protein excretion (g/day)	0.85 ± 0.66	0.77 ± 1.29	0.68
Hematuria score	2.68 ± 1.43	2.24 ± 1.73	0.15
Crea (mg/dl)	0.95 ± 0.50	1.11 ± 0.66	0.02
Ccr (ml/min)	80.53 ± 23.48	65.31 ± 24.58	<0.001
G grade (G0:G1:G2:G3)	14:15:25:14	4:5:19:18	0.04
G grade score	1.57 ± 1.04	2.11 ± 0.92	0.01
T grade (T1:T2:T3)	24:35:9	8:31:7	0.10
T grade score	1.78 ± 0.67	1.98 ± 0.58	0.09
MMI (%)	13.3 ± 5.1	14.4 ± 4.8	0.21
ACE polymorphism (DD:ID:II)	15:25:28	9:22:15	0.49
PAI-1 polymorphism (4G4G:4G5G:5G5G)	29:30:9	11:24:11	0.08

Serum creatinine in mg/dl may be converted to μmol/l by multiplying by 88.4

BP (S) systolic blood pressure, *BP (D)* diastolic blood pressure, *Crea* creatinine, *Ccr* creatinine clearance, *MMI* mesangial matrix index, *ACE* angiotensin converting enzyme, *PAI-1* plasminogen activator inhibitor-1

Table 3 Comparison of clinical characteristics in patients with ≥6 years between onset of proteinuria and renal biopsy and in those with an interval <6 years in mesangioproliferative glomerulopathy without immunoglobulin (Ig)A deposition (N-IgAN)

N-IgAN	<6 years (n = 45)	≥6 years (n = 39)	P value
Age (year)	37.58 ± 18.56	44.769 ± 10.21	0.05
Male:female	26:19	24:15	0.90
Interval from the onset (year)	1.70 ± 1.62	13.92 ± 7.05	<0.001
BP (S) mmHg	126.44 ± 19.87	129.85 ± 14.58	0.15
BP (D) mmHg	73.38 ± 12.13	80.00 ± 10.77	0.04
Urinary protein excretion (g/day)	0.46 ± 0.69	0.55 ± 0.61	0.18
Hematuria score	1.51 ± 1.83	1.13 ± 1.28	0.60
Crea (mg/dl)	0.86 ± 0.28	0.92 ± 0.35	0.40
Ccr (ml/min)	92.79 ± 32.72	85.38 ± 25.72	0.27
G grade (G0:G1:G2:G3)	23:11:7:4	10:17:7:5	0.10
G grade score	0.82 ± 1.00	1.18 ± 0.97	0.06
T grade (T1:T2:T3)	33:7:5	25:7:7	0.60
T grade score	1.38 ± 0.68	1.54 ± 0.79	0.33
MMI (%)	9.30 ± 3.02	10.45 ± 3.67	0.17
ACE polymorphism (DD:ID:II)	5:19:21	3:22:14	0.43
PAI-1 polymorphism (4G4G:4G5G:5G5G)	19:20:6	20:16:3	0.59

Serum creatinine in mg/dl may be converted to μmol/l by multiplying by 88.4

BP (S) systolic blood pressure, *BP (D)* diastolic blood pressure, *Crea* creatinine, *Ccr* creatinine clearance, *MMI* mesangial matrix index, *ACE* angiotensin converting enzyme, *PAI-1* plasminogen activator inhibitor-1

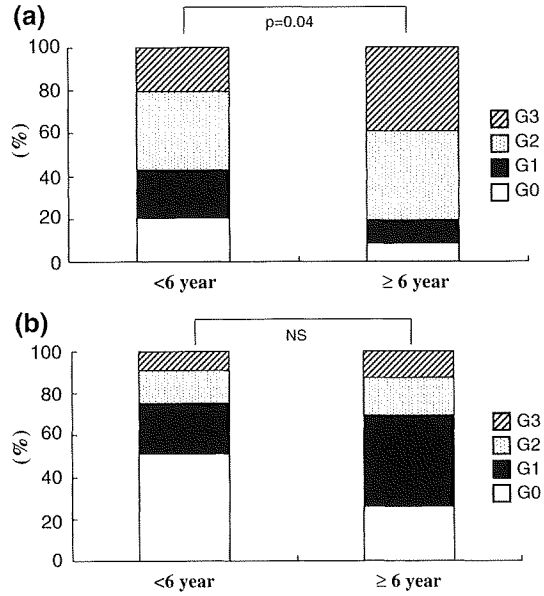

Fig. 3 **a** Degree of pathological glomerular changes are significantly and severely advanced when examined by chi-square test in immunoglobulin (Ig)A nephropathy (*IgAN*) in a time-dependent manner. The ratio of G2+G3 is 80.4% in patients for whom the interval between the onset proteinuria and renal biopsy was ≥6 years. On the other hand, the ratio of G2+G3 was 57.4% in patients with an interval <6 years. **b** Degree of pathological glomerular change is not statistically different according to chi-square test in patients with intervals between the onset of proteinuria and renal biopsy >6 years of mesangioproliferative glomerulopathy without immunoglobulin (Ig)A deposition (N-IgAN) compared with those whose intervals were <6 years. Ratio of G2+G3 was 30.8% in patients with an interval of >6 years. On the other hand, the ratio of G2+G3 was 24.4% in patients with an interval of <6 years

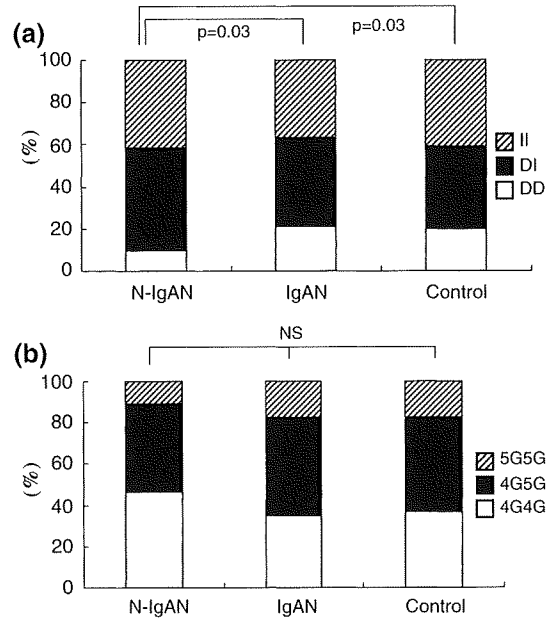

Fig. 4 **a** Frequency of the DD genotype of angiotensin-converting enzyme (*ACE*) was significantly lower in patients with mesangioproliferative glomerulopathy without immunoglobulin (Ig)A deposition (*N-IgAN*) than in those with IgAN or healthy control volunteers. **b** Plasminogen activator inhibitor-1 (PAI-1) gene allele frequency of 4G4G, 4G5G, and 5G5G is similar in patients with mesangioproliferative glomerulopathy without IgA deposition (*N-IgAN*), with IgA nephropathy (*IgAN*), and healthy control volunteers

References

1. Bohle A, Wehrmann M, Bogenschutz O, Batz C, Vogi W, Schmitt H, et al. The long-term prognosis of the primary

glomerulonephritis. A morphological and clinical analysis. Pathol Res Pract. 1992;188:908–24.
2. Kobayashi Y, Tateno S, Hiki Y, Shigematsu H. IgA nephropathy: prognostic significance of proteinuria and histological alterations. Nephron. 1983;34:146–53.
3. Chida Y, Tomura S, Takeuchi J. Renal survival rate of IgA nephropathy. Nephron. 1985;40:189–94.
4. Schena FP. A retrospective analysis of the natural history of primary IgA nephropathy worldwide. Am J Med. 1990;89:209–15.
5. D'Amico G. Influence of clinical and histological features on actuarial renal survival in adult patients with idiopathic IgA nephropathy, membranous nephropathy and membranoproliferative glomerulonephritis: survey of the recent literature. Am J Kidney Dis. 1992;20:315–23.
6. Lee DY, Kim W, Kang SK, Koh GY, Park SK. Angiotensin-converting enzyme gene polymorphism in patients with minimal-change nephrotic syndrome and focal segmental glomerulosclerosis. Nephron. 1997;77:471–3.
7. Gaillard MC, Mahadeva R, Lomas DA. Identification of DNA polymorphisms associated with the V type alpha1-antitrypsin gene. Biochim Biophys Acta. 1999;1444:166–70.
8. Frishberg Y, Toledano H, Becker-Cohen R, Feigin E, Halle D. Genetic polymorphism in paraoxonase is a risk factor for childhood focal segmental glomerulosclerosis. Am J Kidney Dis. 2000;36:1253–61.
9. Yorioka T, Suehiro T, Yasuoka N, Hashimoto K, Kawada M. Polymorphism of the angiotensin converting enzyme gene and clinical aspects of IgA nephropathy. Clin Nephrol. 1995;44:80–5.
10. Yoshida H, Mitarai T, Kawamura T, Kitajima T, Miyazaki Y, Nagasawa R, et al. Role of the deletion of polymorphism of the angiotensin converting enzyme gene in the progression and therapeutic responsiveness of IgA nephropathy. J Clin Invest. 1995;96:2162–9.
11. Harden PN, Geddes C, Rowe PA, McIlroy JH, Boulton-Jones M, Rodger RS, et al. Polymorphisms in angiotensin-converting-enzyme gene and progression of IgA nephropathy. Lancet. 1995;345:1540–2.
12. Suzuki H, Sakuma Y, Kanesaki Y, Eiro M, Asahi K, Sanada H, et al. Close relationship of plasminogen activator inhibitor-1 4G/5G polymorphism and progression of IgA nephropathy. Clin Nephrol. 2004;62:173–9.
13. Cambien F, Poirier O, Lecerf L, Evans A, Cambou JP, Arveiler D, et al. Deletion polymorphism in the gene for angiotensin-converting enzyme is a potent risk factor for myocardial infarction. Nature. 1992;359:641–4.
14. Ludwig E, Corneli PS, Anderson JL, Marshall HW, Lalouel JM, Ward RH. Angiotensin-converting enzyme gene polymorphism is associated with myocardial infarction but not with development of coronary stenosis. Circulation. 1995;91:2120–4.
15. Uemura K, Nakura J, Kohara K, Miki T. Association of ACE I/D polymorphism with cardiovascular risk factors. Human Genet. 2000;107:239–42.
16. Schena FP, D'Altri C, Cerullo G, Manno C, Gesualdo L. ACE gene polymorphism and IgA nephropathy: an ethnically homogeneous study and a meta-analysis. Kidney Int. 2001;60:732–40.
17. Suzuki S, Suzuki Y, Kobayashi Y, Harada T, Kawamura T, Yoshida H, et al. Insertion/deletion polymorphism in ACE gene is not associated with renal progression in Japanese patients with IgA nephropathy. Am J Kidney Dis. 2000;35:896–903.
18. Pei Y, Scholey J, Thai K, Suzuki M, Cattran D. Association of angiotensinogen gene T235 variant with progression of immunoglobin A nephropathy in Caucasian patients. J Clin Invest. 1997;100:814–20.
19. Schimidt SE, Sttier R, Hartung G, Stein J, Bahnisch AJ, Woodroffe AR, et al. No association of converting enzyme insertion/deletion polymorphism with immunoglobulin A glomerulonephritis. Am J Kidney Dis. 1995;26:727–31.
20. Sakai H, Abe K, Kobayashi Y, Koyama A, Shigematsu H, Harada T, et al. Joint Committee of Ministry of Health and Welfare of Japan and Japanese Society of Nephrology. Clinical guidelines of IgA nephropathy. Jpn J Nephrol. 1995;37:417–21.
21. Churg J, Sobin LH. Renal disease: classification and atlas of glomerular disease. Tokyo, Japan: Igaku-shoin; 1982.
22. Walburger DK, Afonina IA, Wydro R. An improved real time PCR method for simultaneous detection of C282Y and H63D mutations in the HFE gene associated with hereditary hemochromatosis. Mutat Res. 2001;432:69–78.
23. Kuriki M, Asahi K, Asano K, Sakurai K, Eiro M, Suzuki H, et al. Steroid therapy reduces mesangial matrix accumulation in advanced IgA nephropathy. Nephrol Dial Transplant. 2003;18:1311–5.
24. Ohishi M, Fujii K, Minamino T, Higaki J, Kamitani A, Rakugi H, et al. A potent genetic risk factor for restenosis. Nature Genet. 1993;5:324–5.
25. Higashimori K, Zhao Y, Higaki J, Kamitani A, Katsuya T, Nakura J, et al. Association analysis of a polymorphism of the angiotensin converting enzyme gene with essential hypertension in the Japanese population. Biochem Biophys Res Commun. 1993;191:399–404.
26. Rigat B, Hubert C, Alhenc-Gelas F, Cambien F, Corvol P, Soubrier F. An insertion/deletion polymorphism in the angiotensin I-converting enzyme gene accounting for half the variance of serum enzyme levels. J Clin Invest. 1990;86:1343–6.
27. Singhal PC, Santiago A, Satriano J, Hays RM, Schlondorff D. Effects of vasoactive agents on uptake of immunoglobulin G complexes by mesangial cells. Am J Physiol. 1990;258:F589–96.

Circ J 2009; **73:** 139–144

Significant Association Between Neutrophil Aggregation in Aspirated Thrombus and Myocardial Damage in Patients With ST-Segment Elevation Acute Myocardial Infarction

Kentaro Arakawa, MD*,¶; Satoshi Yasuda, MD**; Hiroyuki Hao, MD†; Yu Kataoka, MD*; Isao Morii, MD††; Yoichiro Kasahara, MD*; Atsushi Kawamura, MD*; Hatsue Ishibashi-Ueda, MD‡; Shunichi Miyazaki, MD‡‡

Background This study was designed to clarify the relationship between myocardial damage and platelet-neutrophil aggregation in patients with acute myocardial infarction (AMI).

Methods and Results The study group comprised 107 patients with ST-segment elevation AMI, in whom aspiration catheter was used during emergency percutaneous coronary intervention. Patients were divided into 2 groups according to the cellular density of neutrophils in the aspirated sample: group L (n=53), ≤100 neutrophils/0.025 mm^2 thrombus; group H (n=54), >100 neutrophils/0.025 mm^2 thrombus. Myocardial blush grade (MBG) ≤1 and ST-segment resolution (STR) <50% were more frequently found in group H than in group L. Peak creatine kinase level tended to be higher and left ventricular ejection fraction (LVEF) at 6 months after onset was lower in group H than in group L. Multivariate analysis showed that high neutrophil density in aspirated thrombus was an independent predictor of MBG ≤1, STR <50%, and low LVEF at 6 months after onset.

Conclusions Platelet-neutrophil aggregates retrieved from ruptured plaque may be associated with impaired coronary microcirculation and resultant myocardial necrosis/dysfunction. These findings underscore the clinical importance of the interaction between thrombosis and inflammation in the pathogenesis of AMI. (*Circ J* 2009; **73:** 139–144)

Key Words: Inflammation; Lesion; Leukocytes; Myocardial infarction; Thrombus

Patients with acute coronary syndrome (ACS) are characterized by increased platelet activation within the coronary circulation! Thrombus formation at a ruptured or eroded plaque and distal embolization of platelet aggregates eventually lead to myocardial necrosis? Several lines of evidence in experimental ischemia–reperfusion models suggest the pathological significance of neutrophil–platelet interaction in ACS?[3–6] However, the importance of this interaction in humans, especially its in vivo significance, remains unknown.

Thrombus aspiration devices can retrieve thrombi from the culprit coronary lesion and the aspirated samples may provide intraluminal pathological information. In a previous flow cytometric study, neutrophil–platelet aggregate formation indicated activated thrombus,[7] so in the present in vivo study we sought to evaluate the specific role of platelet–neutrophil aggregation in myocardial reperfusion injury, infarct size, and left ventricular (LV) remodeling in patients with ST-segment elevation acute myocardial infarction (STEMI).

Methods

Study Patients

From January 1, 2003 to July 31, 2005, 267 consecutive patients with STEMI were treated with emergency percutaneous intervention (PCI) within 24 h of the onset of chest pain. Inclusion criteria of STEMI were (1) continuous chest pain that lasted >30 min, (2) ST-segment elevation ≥0.1 mV in 2 or more contiguous leads on the 12-lead electrocardiogram (ECG), (3) angiographically detected culprit lesion with diameter stenosis ≥75% and/or Thrombolysis In Myocardial Infarction flow grade 0 or 1, (4) subsequent increase in the serum creatine kinase (CK) level to more than 3-fold of the upper limit of normal.

We used an aspiration device in 147 of the 267 patients. The choice to use aspiration was made by the operator and was based on angiographic images. In total, 40 of the 147 patients without aspirated thrombus were excluded, so in the final analysis, we used the data from 107 patients with STEMI (77 men, 30 women; age 66±12 [mean±standard

(Received June 24, 2008; revised manuscript received August 7, 2008; accepted August 19, 2008; released online December 2, 2008)

**Division of Cardiology, Department of Internal Medicine, National Cardiovascular Center, Suita, **Department of Cardiovascular Medicine, Tohoku University Graduate School of Medicine, Sendai, †Department of Surgical Pathology, Hyogo College of Medicine, Nishinomiya, ††Division of Cardiology, Hokusetsu General Hospital, Takatsuki, ‡Department of Pathology, National Cardiovascular Center, Suita and ‡‡Division of Cardiology, Department of Internal Medicine, Kinki University School of Medicine, Osakasayama, Japan*

¶Current address: Division of Cardiology, Fujisawa City Hospital, Fujisawa, Japan.

Mailing address: Shunichi Miyazaki, MD, Division of Cardiology, Department of Internal Medicine, Kinki University School of Medicine, 377-2 Ohno-Higasgi, Osakasayama 589-8511, Japan. E-mail: smiyazak@med.kindai.ac.jp

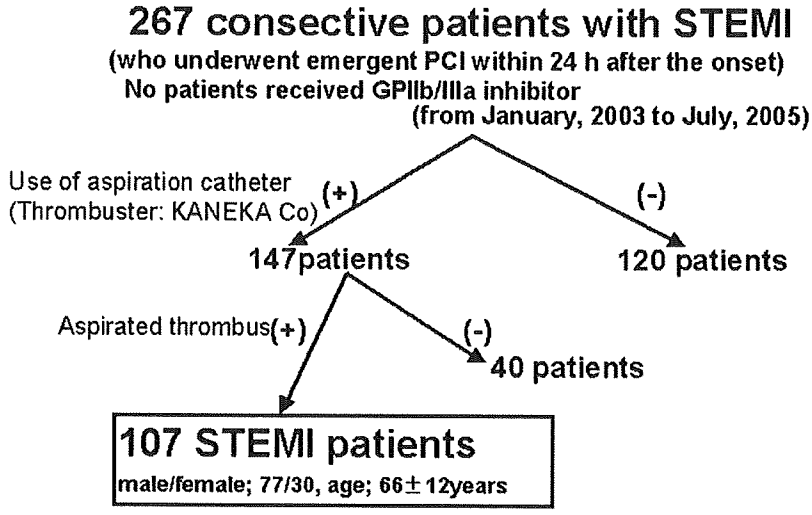

Fig 1. Flowchart of the study. STEMI, ST-segment elevation acute myocardial infarction; PCI, percutaneous intervention. GP, glycoprotein.

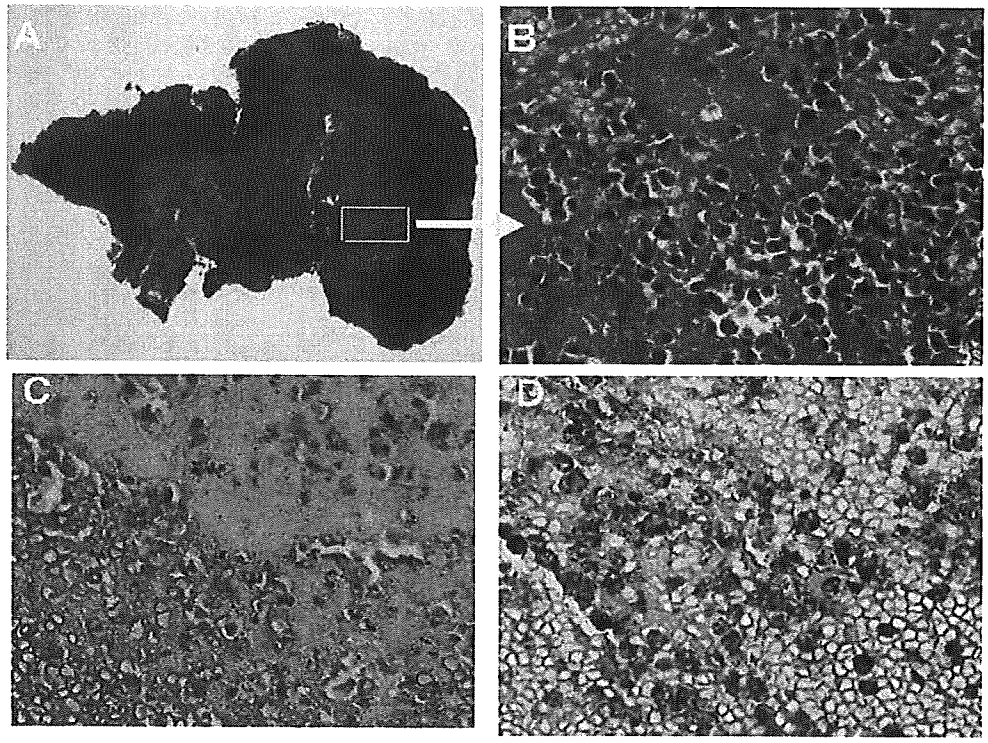

Fig 2. Histological analysis of thrombus burden aspirated from the culprit lesion. (**A**,**B**) Fragment of aspirated thrombus (H&E; A, ×20; B, ×20). (**C**,**D**) Serial sections examined by immunostaining for myeloperoxidase (MPO) and CD66 (C, ×400; D, ×400, respectively). In the quantitative analysis, the numbers of MPO- and CD66-positive cells/0.025 mm^2 were counted in at least 3 high-power fields (×400). The average of the counts from 3 fields with the highest numbers of neutrophils was taken as the neutrophil density.

deviation (SD)] years) (**Fig 1**). Elapsed time to reperfusion was 6.02±0.40 [mean±SD] hours in these patients.

PCI

PCI was performed after intravenous administration of 10,000 IU heparin using a 6 or 7F sheath and catheters. Antiplatelet therapy before PCI consisted of aspirin only, because glycoprotein (GP) IIb/IIIa inhibitors and clopidogrel are not available in Japan. Facilitated thrombolysis with intravenous tissue plasminogen activator (tPA) was performed in 24 patients. After crossing the target lesion with the guidewire, coronary thrombus-aspiration was performed several times (depending on the operator's judgment). Aspiration was performed by 6 or 7F Thrombuster (Kaneka Co, Tokyo, Japan), which is a rapid exchange catheter with a central aspiration lumen and soft, flexible, non-traumatic tip with a large hole that communicates with the central lumen. A 20-ml screw syringe was connected to the proximal hub of the central lumen for thrombus-aspiration. In 23 patients, a distal protection catheter, PercuSurge GuardWire Plus (Medtronic Corp, Santa Rosa, CA, USA) was also used with the aspiration catheter at the operator's

Table 1 Baseline Clinical Characteristics and Coronary Angiographic Findings

	Group L (n=53) Neutrophil density ≤100	Group H (n=54) Neutrophil density >100	P value
Age (years)	67.7±1.6	63.7±1.6	0.083
Gender (male, n (%))	42 (78%)	34 (64%)	0.119
Coronary risk factors, n (%)			
Hypertension	34 (63%)	36 (68%)	0.589
Diabetes mellitus	39 (74%)	32 (63%)	0.235
Hyperlipidemia	38 (70%)	31 (58%)	0.199
Smoking	33 (61%)	27 (54%)	0.092
Family history of CAD	11 (20%)	12 (23%)	0.755
Drugs n (%)			
Anticoagulant	12 (24%)	14 (26%)	0.821
Statins	16 (32%)	11 (21%)	0.194
ACEI/ARB	12 (24%)	6 (12%)	0.152
Ca-antagonists	11 (22%)	16 (30%)	0.344
β-blockers	3 (6%)	6 (11%)	0.334
Nitrates	7 (13%)	3 (6%)	0.210
Inflammatory markers (peripheral blood)			
WBC (/μl)	9,615±455	12,172±451	<0.001
Neutrophil (/μl)	6,609±426	9,218±418	0.001
CRP (mg/dl)	1.12±0.286	0.81±0.286	0.210
Previous MI, n (%)	6 (11%)	8 (14%)	0.424
Pre MI angina, n (%)	28 (52%)	21 (40%)	0.204
Time to reperfusion (h)	4.70±0.54	7.33±0.54	<0.01
Prior tPA, n (%)	16 (30%)	8 (15%)	0.061
Distal protection, n (%)	10 (19%)	13 (24%)	0.512
Killip score 1 vs 2/3/4, n (%)	46/7 (87/13%)	51/3 (94/6%)	0.169
RCA/LAD/LCX/LMT, n (%)	26/21/6/0 (50/39/11/0%)	26/22/5/1 (49/41/9/1%)	0.825
Multivessel disease, n (%)	34 (55%)	26 (58%)	0.431
Pre-reference diameter (mm)	3.42±0.08	3.48±0.09	0.595
Post-reference diameter (mm)	3.41±0.08	3.56±0.09	0.186
Pre-minimum diameter (mm)	0.19±0.05	0.16±0.05	0.748
Post-minimum diameter (mm)	3.20±0.07	3.33±0.08	0.275
Pre %stenosis (%)	96.04±1.34	96.64±1.25	0.748
Post %stenosis (%)	5.03±1.10	6.54±1.21	0.359
Bare metal stent (%)	46 (87%)	48 (89%)	0.970
Final TIMI 0/1/2 vs 3, n (%)	6/47 (11/89%)	7/47 (13/87%)	0.795

Data are mean±SD or median value (25–75th percentile range) or n (%).
CAD, coronary artery disease; ACEI, angiotensin-converting enzyme inhibitor; ARB, angiotensin II receptor blocker; WBC, white blood cell; CRP, C-reactive protein; MI, myocardial infarction; tPA, tissue plasminogen activator inhibitor; RCA, right coronary artery; LAD, left coronary artery; LCX, left circumflex; LMT, left main trunk; TIMI, Thrombolysis In Myocardial Infarction.

discretion. Bare metal stents were implanted in cases of coronary dissection or suboptimal results after balloon angioplasty. Quantitative coronary angiographic analysis was performed by QCA-CMS version 5.0 (MEDIS Medical Imaging Systems, Leiden, The Netherlands).

Assessment of Coronary Microcirculation by ST-Segment Resolution (STR) and Myocardial Blush Grade (MBG)

A 12-lead ECG was recorded immediately (≤30 min) before recanalization, and 1 h after recanalization. ST-segment elevation was measured at 80 ms after the J-point by 2 independent observers who were unaware of all clinical and angiographic findings. The sum of the ST-segment elevations in 3 contiguous leads with the highest ST-segment elevations was calculated. STR was defined as a reduction of at least 50% in ST-segment elevation on ECGs obtained 1 h after recanalization compared with the initial value.[8] In this study group, there were no patients with left bundle-branch block or pacemaker rhythm.

MBG scale was determined by 2 observers, who were unaware of the clinical and angiographic findings, using a previously reported grading scale.[9]

Assessment of LV Function and Infarct Size

LV function was evaluated on right anterior oblique views of left ventriculograms (LVG) obtained immediately and then 6 months after PCI. LV end-diastolic volume index (LVEDVI), and LV ejection fraction (LVEF) were determined by the centerline method (QLV-CMS version 5.0, MEDIS Medical Imaging Systems).

Blood samples were obtained on admission and at 3-h intervals until the CK level peaked and that value was used as the enzymatic marker of infarct size.

Measurement of Neutrophil Density in Aspirated Thrombi

The thrombi obtained by aspiration were immediately fixed in 10% buffered formalin solution for 6 h at 4°C and embedded in paraffin. Sections (4-μm thick) were stained with hematoxylin-eosin, and serial sections were immunostained for myeloperoxidase (MPO) and CD66 to identify neutrophils. After deparaffinization, tissues were pretreated with heat-induced epitope retrieval and the endogenous peroxidase activity was blocked with 3% hydrogen peroxidase in methanol for 10 min. The sections were then incubated with a monoclonal antibody against human CD66 (DAKO Japan, Kyoto, Japan) and a polyclonal antibody against human MPO (DAKO Japan). Antibodies were used at a dilution of 1:50 and 1:600, respectively. Sections were washed with phosphate-buffered saline followed by incubation with Envision+ (DAKO Japan) for 30 min. After

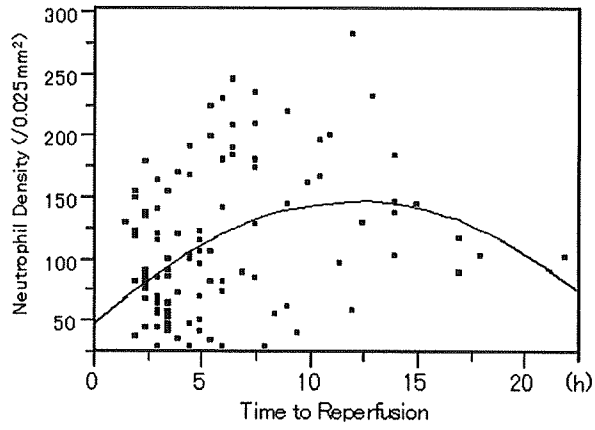

Fig 3. Association between neutrophil density and time to reperfusion. Regression analysis showing that the curve has a peak of neutrophil density around 13 h ($P<0.01$, $r=0.285$); the increased neutrophil density was not a simple function of time.

further washes, the sections were incubated with 0.005% 3,3'diaminobenzidine solution diluted with 5% hydrogen peroxide and counterstained with Meyer's hematoxylin. As the negative control for immunostaining, normal mouse immunoglobulin G was used instead of the primary antibody. The tissue from a lung abscess obtained at autopsy was used as the positive control.

The following quantitative analysis was performed by a pathologist who was unaware of the clinical information. As shown in **Fig 2**, the number of neutrophils in each aspirated thrombus was counted in a 0.025-mm^2 recutanglar region of interest (ROI). The neutrophil density in the thrombus was taken as the average of 3 ROI.

Statistical Analysis

Data are expressed as mean ± SD for continuous variables and as percentages for categorical variables. For testing of significance, continuous variables were compared using Student's t-test, and categorical data were compared using the chi-square test. To examine the relationship between neutrophil density and time to reperfusion, we constructed a quadratic regression curve and also assessed linear trend by analysis of variance. The variables included the clinical baseline (age, gender, medications, coronary risk factors, time to reperfusion, systolic blood pressure and heart rate on admission, peripheral inflammation data, culprit lesion, previous angina, the use of thrombolytic agents, and distal protection) and the neutrophil count in thrombi. Univariate and multivariate analyses were performed by logistic regression to determine independent predictors of impaired myocardial reperfusion and LV dysfunction (LVEF<45%) 6 months after onset. In this analysis, factors associated with the dependent variable at $P<0.20$ in the univariate analysis were entered into the multivariate model and eliminated using a backward procedure. A P-value<0.05 was regarded as statistically significant. All analyses were performed using the JUMP 5.1 software (SAS Institute, Cary, NY, USA).

Results

Neutrophils were detected in all of the aspirated thrombi. Patients were divided into 2 groups on the basis of the median density of all samples, which was 100.33 (27.33–287.33): group L, neutrophil density ≤100/0.025 mm^2 (n=53), and group H, neutrophil density >100/0.025 mm^2 (n=54).

Comparison of Patients' Characteristics and Angiographic Findings

Clinical characteristics and angiographic findings are summarized in **Table 1**. The majority of the parameters, with the exception of the white blood cell (WBC) neutrophil counts in peripheral blood, and the time to reperfusion, were similar between groups. The relationship between neutrophil density and time to reperfusion was not linear and the regression curve peaked at approximately 13 h (**Fig 3**). Additionally, there was not a linear relationship even when the patients were divided into 4 groups according to time to reperfusion: <6 h, 93±7/0.025 mm^2 (n=66); 6–12 h, 148±9/0.025 mm^2 (n=31); 12–18 h, 138±20/0.025 mm^2 (n=8); 18–24 h, 102±39/0.025 mm^2 (n=2).

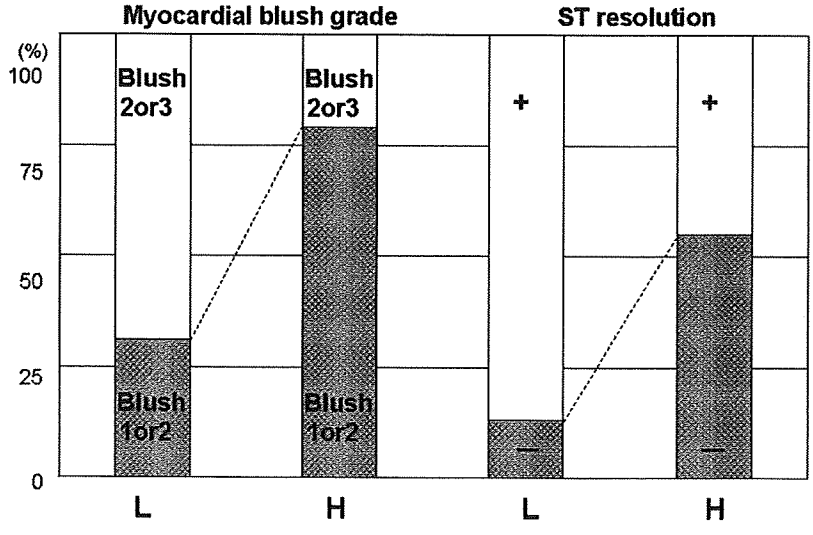

Fig 4. Comparison of myocardial reperfusion injury between group H (>100 neutrophils/0.025 mm^2) and group L (≤100 neutrophils/0.025 mm^2). **(Left)** Myocardial blush grade. Open bar indicates blush grade 2 or 3 and solid bar indicates blush grade 0 or 1. **(Right)** ST-segment resolution (STR). Open bar indicates STR and solid bar indicates no STR.

Table 2 Comparison of Groups L and H for Left Ventricular Function

	Group L (n=53)	Group H (n=54)	P value
LVEDVI (ml/m²)			
Immediately after PCI	67.2±2.5	71.7±2.6	0.230
6 months after PCI	72.9±3.1	78.2±2.9	0.215
LVEF (%)			
Immediately after PCI	43.6±1.2	41.4±1.2	0.186
6 months after PCI	47.1±1.5	42.4±1.4	0.021

Data are mean±SD.
LVEDVI, left ventricular end-diastolic volume index; PCI, percutaneous coronary intervention; LVEF, left ventricular ejection fraction.

Table 3 Multivariate Analysis for the Incidence of Myocardial Reperfusion Injury and Left Ventricular Dysfunction

	OR (95%CI)	P value
Blush Grade 0 or 1		
LAD lesion	0.324 (0.118–0.826)	0.0216
Neutrophil count in thrombi	9.430 (3.777–25.912)	<0.0001
Absence of preceding tPA	2.450 (0.827–7.712)	0.1120
No ST-segment resolution		
RCA lesion	0.438 (0.163–1.117)	0.0898
Neutrophil count in thrombi	3.272 (1.249–9.070)	0.0180
Time to reperfusion	76.960 (6.595–1,385.694)	0.0013
LVEF <45% at 6 months		
Neutrophil count in thrombi	5.683 (2.044–17.474)	0.0014
LAD lesion	2.296 (0.830–6.728)	0.1164
Systolic BP on admission	0.024 (0.001–0.425)	0.0157

OR, odds ratio; CI, confidence interval; BP, blood pressure. Other abbreviations see in Tables 1,2.

Impaired Coronary Microcirculation, Myocardial Damage, and Myocardial Function

Impaired coronary microcirculation, defined as MBG of 0 or 1 (79% and 31%, respectively) and no STR (55% and 13%, respectively) occurred more frequently in group H than in group L (P<0.001) (**Fig 4**). Also, peak CK levels tended to be higher in group H than in group L (4,387± 400 U/L vs 3,284±403 U/L, P=0.05).

Volumetric data immediately after and at 6 months after PCI are summarized in **Table 2**. LVG was performed at both time points in 38 patients in group L and in 42 patients in group H. LVEDVI and LVEF were similar for the 2 groups immediately after PCI, but at 6 months after the onset of AMI, LVEF was significantly lower in group H than in group L while LVEDVI remained similar in both groups.

Multivariate Analysis

To investigate which clinical variables and risk factors were associated with impaired coronary microcirculation and myocardial damage, we performed univariate and multivariate analyses (**Table 3**). Neutrophil density in thrombus was a common independent predictor for MBG 0 or 1, no STR, and LVEF<45% at 6 months. A significant association was found between LAD lesions and MBG 0 or 1, between time to reperfusion and no STR, and between low systolic blood pressure and LVEF<45% at 6 months. However, after incorporation of neutrophil count in thrombi into the multivariate regression model, the peripheral WBC and neutrophil count were not associated factors.

Discussion

To our knowledge, this is the first report of an analysis of the immunohistology of aspirated thrombi obtained from the culprit lesions in patients with STEMI. The major finding is that high neutrophil density in aspirated thrombus is associated with impaired coronary microcirculation, consequent myocardial damage (elevated CK level), and LV dysfunction.

A growing body of evidence suggests that inflammation plays an important role in ACS, followed by progression of atherosclerosis, plaque rupture and coronary occlusion because of thrombus formation. Aspiration devices have facilitated the recent study of aspirated thrombi, thus providing novel information regarding the histology of the culprit lesions.

Neutrophils stained with anti-MPO and anti-CD66 antibodies were detected in all of the aspirated thrombi in the present study (**Fig 2**). Local accumulation of neutrophils may be associated with increased platelet activity, as reported in a flow cytometric study[3] Neutrophil aggregation may be also involved in the primary etiology of increased platelet activity in the process of ACS. Activated neutrophils are reported to enhance platelet aggregation and thromboxane release in a P-selectin–P-selectin glycoprotein ligand-1 dependent manner, followed by an adhesion-strengthening interaction mediated by the β 2-integrin and Mac-1[4,10,11] Neutrophil-platelet aggregates are vehicles for the local delivery of surface-bound tissue factor, coagulation factor Xa and fibrinogen, each of which is a key component of the local coagulation response![12]

A recent randomized trial of patients with STEMI demonstrated that manual thrombus aspiration improved myocardial reperfusion, as compared with conventional PCI![13] The present study focused on the characteristics of aspirated thrombus and demonstrated that peak CK level tended to be higher in patients in which thrombus contained >100 neutrophils/0.025 mm² compared with those in which thrombus contained ≤100/0.025 mm². Moreover, although we did not obtained follow-up volumetric data in all patients

and medical treatments, especially the usage of statins, angiotensin-converting enzyme inhibitors and angiotensin II receptor blockers, were not totally matched between the 2 groups, the paired data demonstrated that LVEF at 6 months after the onset of AMI was significantly different between the 2 groups (**Table 2**). Elevated peripheral inflammatory markers, which are associated with progression of myocardial damage after recanalization in patients with STEMI,[14–18] were not independent predictors for impaired coronary microcirculation and myocardial damage after inclusion of neutrophil count in thrombi into a multivariate model (**Table 3**). These findings indicate an important association between intraluminal platelet–neutrophil aggregates and clinical outcome following reperfusion therapy. Platelet–neutrophil aggregates could cause distal embolization by plugging the microvascular structures and activating the inflammatory cascade, leading to myocardial injury, probably because of increased production of reactive oxidants and diffusible radical species![19]

Several experimental studies have shown that inhibition of neutrophil–platelet aggregation or neutrophil adhesion to endothelium with monoclonal antibodies can reduce infarct size; however, the studies in humans have been disappointing?[20–24] One possible explanation for the failure of anti-neutrophil therapy in humans is the pathway of administration. Systemic drug administration may not result in sufficient concentration to modulate local inflammation in the culprit lesion. In addition to local administration, a successful strategy against reperfusion injury may require targeting several pathways at once, rather than attempting to block a single final pathway. In fact, in a mouse AMI model, combined antibody therapy targeting both P-selectin and intercellular adhesion molecule-1 achieved a much greater reduction in infarct size, improved the LVEF, and regional myocardial blood flow compared with administration of either one of the antibodies alone?[25]

In conclusion, platelet–neutrophil aggregates retrieved from ruptured plaques may be associated with impaired coronary microcirculation and resultant myocardial necrosis/dysfunction. Although further prospective validation is needed, these findings indicate the clinical importance of the interaction between the pathways involved in thrombosis and inflammation in the pathogenesis of AMI.

Disclosures

None.

References

1. Libby P, Ridker PM, Maseri A. Inflammation and atherosclerosis. *Circulation* 2002; **105:** 1135–1143.
2. Davies MJ, Thomas AC, Knapman PA, Hangartner JR. Intramyocardial platelet aggregation in patients with unstable angina suffering sudden ischemic cardiac death. *Circulation* 1986; **73:** 418–427.
3. Merten M, Thiagarajan P. P-selectin expression on platelets determines size and stability of platelet aggregates. *Circulation* 2000; **102:** 1931–1936.
4. Evangelista V, Manarini S, Coller BS, Smyth SS. Role of P-selectin, beta 2-integrins, and Src tyrosine kinases in mouse neutrophil-platelet adhesion. *J Thromb Haemost* 2003; **1:** 1048–1054.
5. Kumar A, Villani MP, Patel UK, Keith JC Jr, Schaub RG. Recombinant soluble form of PSGL-1 accelerates thrombolysis and prevents reocclusion in a porcine model. *Circulation* 1999; **99:** 1363–1369.
6. Arai M, Lefer DJ, So T, Dipaula A, Aversano T, Becker LC. An anti-CD18 antibody limits infarct size and preserves left ventricular function in dogs with ischemia and 48-hour reperfusion. *J Am Coll Cardiol* 1996; **27:** 1278–1285.
7. Michelson AD, Bernald MR, Krueger LA, Valeri CR, Furman MI. Circulating monocyte-platelet aggregates are a more sensitive marker of in vivo platelet activation than platelet surface activation. *Circulation* 2001; **104:** 1533–1537.
8. Matetzky S, Novikov M, Gruberg L, Freimark D, Feinberg M, Elian D, et al. The significance of persistent ST elevation versus early resolution of ST segment elevation after primary PTCA. *J Am Coll Cardiol* 1999; **34:** 1932–1938.
9. Van't Hof AWJ, Liem A, Suryapranata H, Hoorntje JCA, de Boer M, Zijilstra F. Angiographic assessment of myocardial reperfusion in patients treated with primary angioplasty for acute myocardial infarction. *Circulation* 1998; **97:** 2302–2306.
10. Faraday N, Scharpf RB, Dodd-o JM, Martinez EA, Rosenfeld BA, Dorman T. Leukocytes can enhance platelet-mediated aggregation and thromboxane release via interaction of P-selectin glycoprotein ligand 1 with P-selectin. *Anesthesiology* 2001; **94:** 145–151.
11. de Gaetano G, Cerletti C, Evangelista V. Recent advances in platelet-polymorphonuclear leukocyte interaction. *Haemostasis* 1999; **29:** 41–49.
12. Barnard MR, Linden MD, Frelinger AL III, Li Y, Fox ML, Furman MI, et al. Effects of platelet binding on whole blood flow cytometry assays of monocyte and neutrophil procoagulant activity. *J Thromb Haemost* 2005; **3:** 2563–2570.
13. Svilaas T, Vlaar PJ, van der Horst IC, Diercks GF, de Smet BJ, van der Heuvel AF, et al. Thrombus aspiration during primary percutaneous coronary intervention. *N Engl J Med* 2008; **358:** 557–567.
14. Kosuge M, Kimura K, Ishikawa T, Shimizu T, Takemura T, Tsukahara K, et al. Relation between white blood cell counts and myocardial reperfusion in patients with recanalized anterior acute myocardial infarction. *Circ J* 2004; **68:** 526–531.
15. Barron HV, Cannon CP, Murphy SA, Braunwald E, Gibson M. Association between white blood cell count, epicardial blood flow, myocardial perfusion, and clinical outcomes in the setting of acute myocardial infarction. *Circulation* 2000; **102:** 2329–2334.
16. Kirtane AJ, Bui A, Murphy SA, Barron HV, Gibson CM. Association of peripheral neutrophilia with adverse angiographic outcomes in ST-elevation myocardial infarction. *Am J Cardiol* 2004; **93:** 532–536.
17. Takahashi T, Hiasa Y, Ohara Y, Miyazaki S, Ogura R, Suzuki N, et al. Relationship of admission neutrophil count to microvascular injury, left ventricular dilation, and long-term outcome in patients treated with primary angioplasty for acute myocardial infarction. *Circ J* 2008; **72:** 867–872.
18. Kruk M, Przyłuski J, Kalińczuk Ł, Pregowski J, Deptuch T, Kadziela J, et al. Association of non-specific inflammatory activation with early mortality in patients with ST-elevation acute coronary syndrome treated with primary angioplasty. *Circ J* 2008; **72:** 205–211.
19. Tóth-Zsámboki E, Horváth E, Vargova K, Pankotai E, Murthy K, Zsengellér Z, et al. Activation of poly (ADP-ribose) polymerase by myocardial ischemia and coronary reperfusion in human circulating leukocytes. *Mol Med* 2006; **12:** 221–228.
20. Mertens P, Maes A, Nuyts J, Belmans A, Desmet W, Esplugas E, et al. Recombinant P-selectin glycoprotein ligand–immunogloblin, a P-selectin antagonist, as an adjunct to thrombolysis in acute myocardial infarction: The P-selectin antagonist limitingmyonecrosis (PSALM) trial. *Am Heart J* 2006; **152:** 125.e1–125.e8.
21. Baran KW, Nguyen M, McKendall GR, Lambrew CT, Dykstra G, Palmeri ST, et al. Double-blind, randomized trial of anti-CD18 antibody in conjunction with recombinant tissue plasminogen activator for acute myocardial infarction. *Circulation* 2001; **104:** 2778–2783.
22. Collaborative Organization for Rheoth RX Evaluation (CORE) Investigators. Effect of Phoeth Rx on mortality, morbidity, left ventricular function, and infarct size in patients with acute myocardial infarction. *Circulation* 1997; **96:** 192–201.
23. Faxon DP, Gibbons RJ, Chronos NA, Gurbel PA, Sheehan F; HALT-MI investigators. The effect of blockade of the CD11/CD18 integrin receptor on infarct size in patients with acute myocardial infarction treated with direct angioplasty: The results of the HALT-MI study. *J Am Coll Cardiol* 2002; **40:** 1199–1204.
24. Theroux P, Chaitman BR, Danchin N, Erhardt L, Meinertz T, Schroeder JS, et al. Inhibition of the sodium-hydrogen exchanger with cariporide to prevent myocardial infarction in high-risk ischemic situations: Main results of the GUARDIAN trial. *Circulation* 2000; **102:** 3032–3038.
25. Fukushima S, Coppen SR, Varela-Carver A, Yamahara K, Sarathchandra P, Smolenski RT, et al. A novel strategy for myocardial protection by combined antibody therapy inhibiting both P-selectin and intercellular adhesion molecule-1 via retrograde intracoronary route. *Circulation* 2006; **114**(Suppl): I-251–I-256.